INFORMATION TO USERS

This reproduction was made from a copy of a document sent to us for microfilming. While the most advanced technology has been used to photograph and reproduce this document, the quality of the reproduction is heavily dependent upon the quality of the material submitted.

The following explanation of techniques is provided to help clarify markings or notations which may appear on this reproduction.

1. The sign or "target" for pages apparently lacking from the document photographed is "Missing Page(s)". If it was possible to obtain the missing page(s) or section, they are spliced into the film along with adjacent pages. This may have necessitated cutting through an image and duplicating adjacent pages to assure complete continuity.

2. When an image on the film is obliterated with a round black mark, it is an indication of either blurred copy because of movement during exposure, duplicate copy, or copyrighted materials that should not have been filmed. For blurred pages, a good image of the page can be found in the adjacent frame. If copyrighted materials were deleted, a target note will appear listing the pages in the adjacent frame.

3. When a map, drawing or chart, etc., is part of the material being photographed, a definite method of "sectioning" the material has been followed. It is customary to begin filming at the upper left hand corner of a large sheet and to continue from left to right in equal sections with small overlaps. If necessary, sectioning is continued again — beginning below the first row and continuing on until complete.

4. For illustrations that cannot be satisfactorily reproduced by xerographic means, photographic prints can be purchased at additional cost and inserted into your xerographic copy. These prints are available upon request from the Dissertations Customer Services Department.

5. Some pages in any document may have indistinct print. In all cases the best available copy has been filmed.

University Microfilms International
300 N. Zeeb Road
Ann Arbor, MI 48106

1320505

NAIR, N. RAMACHANDRAN

ELECTROCHEMICAL CORROSION STUDIES ON COATED SHEET STEEL

UNIVERSITY OF NEVADA, RENO M.S. 1982

University
Microfilms
International 300 N. Zeeb Road, Ann Arbor, MI 48106

PLEASE NOTE:

In all cases this material has been filmed in the best possible way from the available copy. Problems encountered with this document have been identified here with a check mark __✓__.

1. Glossy photographs or pages _____
2. Colored illustrations, paper or print _____
3. Photographs with dark background _____
4. Illustrations are poor copy _____
5. Pages with black marks, not original copy _____
6. Print shows through as there is text on both sides of page _____
7. Indistinct, broken or small print on several pages ✓
8. Print exceeds margin requirements _____
9. Tightly bound copy with print lost in spine _____
10. Computer printout pages with indistinct print _____
11. Page(s) _____ lacking when material received, and not available from school or author.
12. Page(s) _____ seem to be missing in numbering only as text follows.
13. Two pages numbered _____. Text follows.
14. Curling and wrinkled pages _____
15. Other _____

University
Microfilms
International

University of Nevada

Reno

Electrochemical Corrosion Studies on Coated Sheet Steel

A thesis submitted in partial fulfillment of the requirements for the degree of Master of Science in Metallurgical Engineering

by

N.Ramachandran Nair

December 1982

The thesis of N.Ramachandran Nair is approved :

Thesis Adviser

Department Chairman

Dean, Graduate School

University of Nevada

Reno

December 1982

ABSTRACT

The corrosion of zinc- and zinc- alloy coated steels was measured by electrochemical methods in 0.1 N and 1.0 N sodium chloride solution. The purpose was to develop improved testing methods for quality control and development of improved coatings.

In order to study the effect of galvanic coupling between coating and substrate steel, a scribe was machined in the coating to expose the steel which, in turn, was exposed to electrolyte. The purpose was to simulate service conditions wherein coating may be mechanically damaged. It was found that corrosion rate of coating, regardless of composition, increased in deaerated solutions. In solutions containing dissolved oxygen this was not always the case because of the non - reproducibility of migration of dissolved oxygen to corroding surface.

Although it was difficult to distinguish between pure zinc coatings, demarcation between pure zinc- and alloy- coatings was possible.

TABLE OF CONTENTS

Chapter I

INTRODUCTION

Corrosion may be defined as the deterioration of material because of reaction with its environment (1). The annual cost of corrosion and of protection against corrosion in this country is estimated at several billion dollars.

The major cause of corrosion in automobiles is the deicing salts used on highways. The industry is responding to the situation by developing new coatings to improve the galvanised (pure zinc) coatings which have been predominant. The result has been a variety of new alloys, primarily zinc - based. This in turn necessitated the development of procedures for corrosion testing and quality control. The present project was initiated to address this specific need. Corrosion rate was studied using electrochemical polarisation with a view to develop a testing procedure which will be inexpensive and simple, if necessary, to be used for quality control and coating development.

The corrosion rate of a metal may change continuously with time because of several factors (2). Among these may be included changes in the nature of insoluble corrosion products which may accumulate on

the surface; or changes in composition of environment because of corrosion process; or changes in the real area of the metal surface due to such effects as preferred grain boundary attack. The weight loss of a metal over a time interval does not yield the true corrosion rate, but rather produces an average rate over the interval. Intermittently removing the sample for weight change measurements affects the subsequent corrosion rate upon re - exposure to the environment. Chemical analysis of the solution also presents difficulties particularly when the rate changes markedly with time or when corrosion products are insoluble. These methods are also tedious and may not be sufficiently sensitive to detect changes during the early stages of corrosion.

It is imperative that corrosion rate in a system be measured without the method itself disturbing the corrosion process. Electrochemical methods achieve this objective. The obvious advantage of electrochemical testing is that it may serve as an alternative to the salt spray accelerated test. The latter consists of spraying the specimen in an enclosed chamber with 5% sodium chloride solution (3). Corrosion attack is evaluated by any one of the several specified methods (4,5,6). Further, the

electrochemical method is sensitive to coating degradation as evidenced by the work (7) on anodised coatings of aluminium, and on phosphate - coated steel (8). Thus the choice of the same tool of investigation assumes special significance in relation to the project at hand.

Electrochemical priciples

A simple way to understand corrosion process is to consider it as an electrochemical reaction (1). An electrochemical reaction can be divided into two or more partial reactions of oxidation and reduction. An oxidation or anodic reaction involves an increase in valence or production of electrons while a decrease in valence or consumption of electrons is indicated in the reduction or cathodic reaction. Consider a metal in contact with a solution containing its own ions. Such a situation is represented b y the equation

$$M = M^{z+} + z\,e^{-} \quad \ldots.(1)$$

At equilibrium, rates in forward as well as reverse directions are equal and the net rate is zero. Since electrons are being transferred, it is possible to represent reaction rates by current density. From Faraday's law, the amount of metal reduced or oxidised

is given by

$$W = \frac{I\ t\ A}{z\ F}$$

where

I = current

t = time of reaction

A = atomic weight

z = valency

from which the rate of reaction is found to be proportional to the current. At equilibrium the rates of forward and reverse reactions are equal and the corresponding current density is called the exchange current density. The reversible electrode potential is known to vary with the concentration of ions, and these potentials, when reactants are at standard states, comprise the electromotive series.

However, it is not always possible to have the above situation in practice since some reducible ions are usually present in the solution. In this case the equilibrium is represented by

$$M = M^{z+} + z\ e^- \qquad E^1 \text{ (anodic)} \quad ..(2)$$

$$X^{z+} + z\ e^- = X \qquad E^2 \text{ (cathodic)}. (3)$$

where M represents the metal and X any reducible ion in the electrolyte. The free energy change accompanying the above reaction is related to the electrochemical potential by the equation

$$\Delta G = - z\ F\ E \quad ..... (4)$$

where z is the number of electrons involved, and F is the Faraday constant (=96500 coulombs). Equations (2) and (3) represent the two half - cell reactions with M and X being the anodic and cathodic reactants respectively. When M and X are coupled together, the more electrochemically negative element will act as anode and the other as cathode and the algebraic sum of the standard electrode potentials will indicate the direction of the overall cell reaction since a negative value of change in free energy as calculated by the above equation will indicate the most feasible direction.

Figure 1 shows the variation of electrode potential with current density when metal M is in contact with the electrolyte. The i_o values represent the exchange current density where forward and reverse reactions are in equilibrium. The firm lines portray the polarisation phenomenon for both forward and reverse directions. It is not possible in practice to obtain these polarisation curves because of the difficulty in isolating a single specie in an electrolyte. Figure 1 is actually a juxtaposition of the behaviour of two species in an electrolyte, either behaviour comprising of its own particular oxidation and reduction reactions.

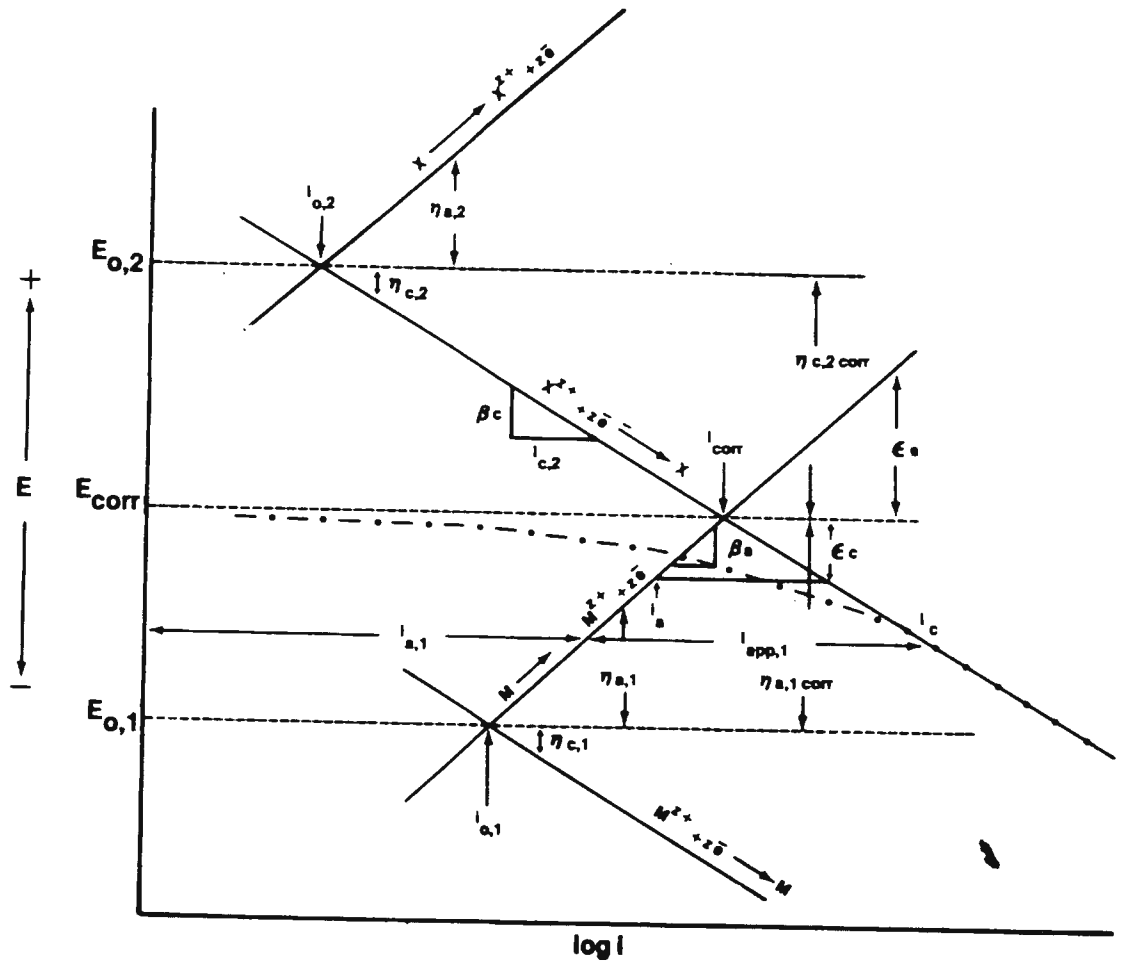

Figure 1. Electrochemical mechanism of corrosion

The condition of equality in rates of oxidation and reduction dictate that there be an equilibrium between the two. This is represented by the corrosion potential E_{corr} and the corresponding corrosion current density. Therefore i_{corr} is a measure of the corrosion rate of metal M under the particular environment.

The firm lines to the right of i_{corr} represent the situation when current is applied to the system. The applied current is the difference between the cathodic and anodic currents, i.e.,

$$i_{app} = i_c - i_a \quad \ldots \quad (5)$$

as shown in Figure 1. It may be noted that the system may be anodically ($M = M^{z+} + z\, e^-$) or cathodically ($X^{z+} + z\, e^- = X$) polarised depending on the direction of current flow, the overvoltages being designated by ε to distinguish from redox overvoltage. By polarisation it is possible to arrive at a value for β by measuring the slope of the voltage - current plot.

The situation arising out of a deviation from equilibrium is called polarisation. Two types of polarisation are encountered most frequently. They are concentration and activation polarisation. As reducible ions are consumed at the electrode surface the rate of migration to the surface becomes

controlling. There is a maximum or limiting current which can be sustained by ionic diffusion. This limiting current is given by

$$i_L = \frac{D\ z\ F\ C_b}{\delta(1 - t)}$$

where D = diffusivity of ionic specie

t = transport number

C_b = bulk concentration

δ = thickness of diffusion layer

The deviation in potential from equilibrium potential brought about by concentration effects is termed concentration overvoltage and is given by (Figure 2)

$$\eta_c = \frac{z\ F}{2.303\ RT} \log\left(1 - \frac{i}{i_L}\right)$$

The second type of polarisation (Figure 3) is encountered when a reaction is associated with a rate - determining step other than diffusion. This is termed activation polarisation and is given by

$$\eta_a = \pm\ \beta \log \frac{i}{i_o}$$

where η_a = activation polarisation

β = Tafel constant

i_o = exchange current density

Galvanic corrosion

Figure 4 illustrates the mechanism of galvanic coupling (1). The normal corrosion

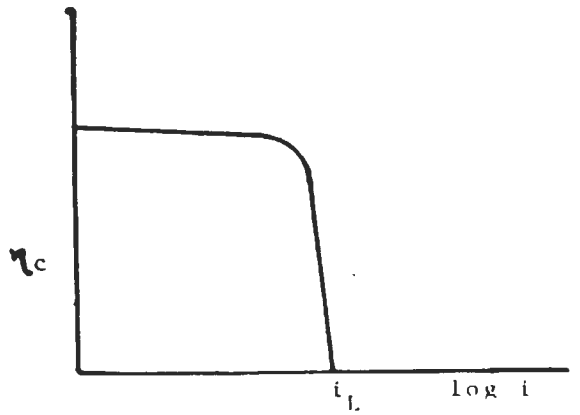

Figure 2. Concentration polarisation

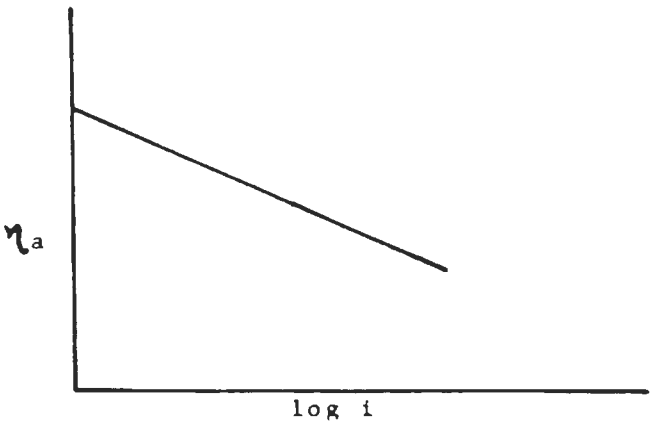

Figure 3. Activation polarisation

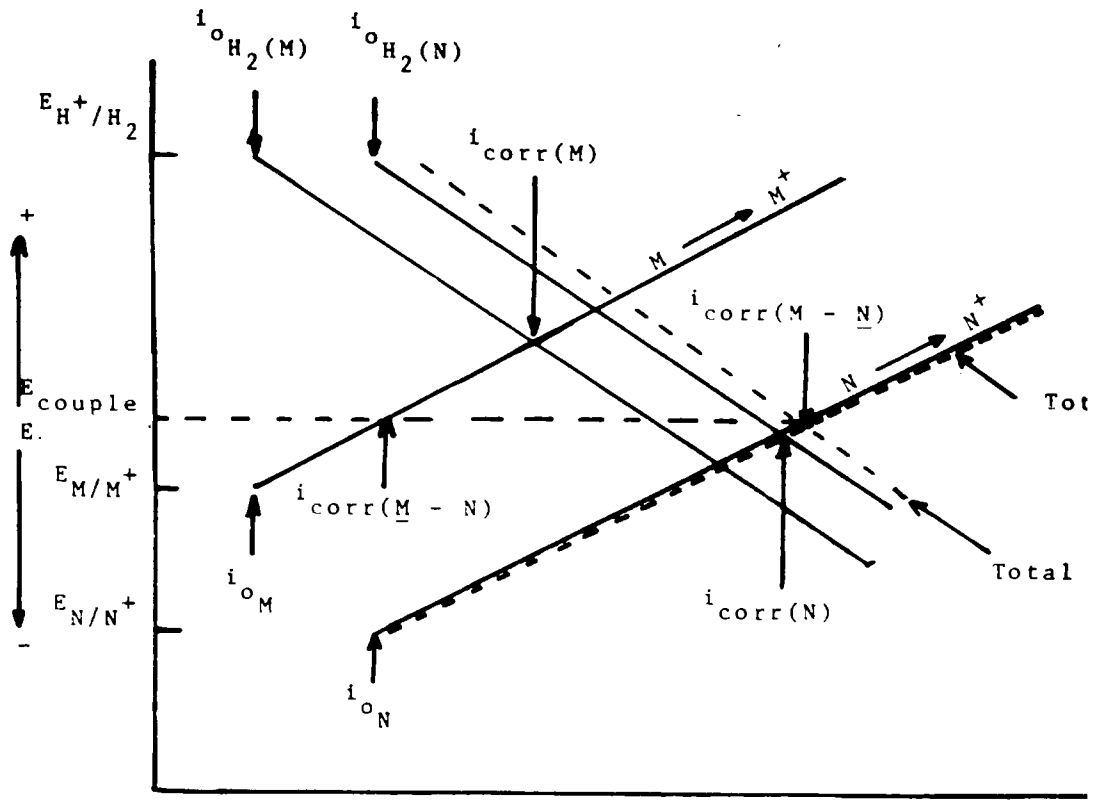

Figure 4. Electrochemical mechanism of galvanic corrosion(After Fontana and Greene(1))

- $\underline{N}$)

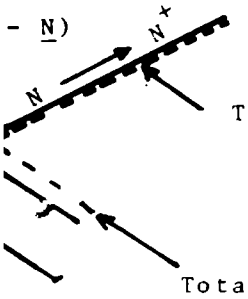

Total oxidation rate

Total reduction rate

)

.sm of galvanic
. and Greene(1))

behaviour of two metals M and N are depicted by the firm lines. While Figure 1 is a juxtaposition of corrosion behaviour of two species of ions, namely, metal M and reducible specie X, Figure 4 represents the juxtaposition of two such couples each of which consists of two species. In the present instance the couples are M - hydrogen and N - hydrogen. Together they form the galvanic couple. Galvanic corrosion is a type of corrosion which occurs when two dissimiliar metals are in electrical contact in the presence of an electrolyte. The metal with the more electronegative corrosion potential becomes an anode and the noble metal becomes the cathode. For equilibrium, the total oxidation rate should equal the total reduction rate. These are represented by the dotted lines which are the algebraic sum of each of the oxidation and reduction curves. The point of intersection signifies equality in rates and determines the galvanic corrosion current. This current is found to be higher than the corrosion current of the more electronegative metal. In other words, the corrosion rate of metal N is accelerated from $i_{corr(N)}$ to $i_{corr(M-\underline{N})}$ while that of M is decreased from $i_{corr(M)}$ to $i_{corr(\underline{M}-N)}$. Metal N is known as sacrificial anode. This is the basis of galvanic protection of steel. The coating here is the

anode and steel the cathode, whenever the steel substrate becomes exposed. The coating becomes the sacrificial anode and corrodes, while steel is protected.

Determination of corrosion current

Both anodic and cathodic polarisation are employed to obtain the polarisation curves in Figure 1. Cathodic polarisation data are more reversible, less time - dependent, and do not cause surface dissolution. If the potential of the electrode is plotted against the logarithm of applied current, a figure similiar to that shown in Figure 1 is obtained. The chain - dotted curve is non - linear at low currents, but at higher currents becomes linear. Applied cathodic current is equal to the difference between the current corresponding to the reduction process and that corresponding to the oxidation process. At relatively high applied current densities, the applied current approaches the total cathodic current, since the corresponding total anodic current becomes negligible. This region of linearity is referred to as the Tafel region. To determine the corrosion rate, the Tafel region is extrapolated to the corrosion potential. At the corrosion potential, the rate of reduction is equal to the rate of metal dissolution, and this point

corresponds to the corrosion rate of the system expressed in terms of current density.

The advantages of this method are many (1). Rapid measurement of corrosion rate is possible. Very low corrosion rates can be measured. Also corrosion rate of structures which cannot be visually inspected or subjected to weight - loss tests may be evaluated However, there are a few restrictions. To ensure reasonable accuracy, the Tafel region must extend over a range of at least one order of magnitude. In many systems this cannot be achieved because of extraneous effects. Also the method can only be employed in systems containing one reduction process, since the Tafel region is usually distorted if more than one reduction occurs.

The second method, which is known as linear polarisation resistance method, is based on the fact that within a few mV of the corrosion potential, the applied current density is a linear function of overvoltage, and the slope of this linear curve is related to corrosion rate.

Referring to Figure 1, at the corrosion potential E_{corr} (10),

$$i_{o,1} = i_{corr} \exp\left(\frac{\eta_{a,1\ corr}}{b_{a,1}}\right)$$

$$i_{o,2} = i_{corr} \exp\left(\frac{\eta_{c,2\ corr}}{b_{c,2}}\right)$$

where $b = \beta / 2.303$

Defining $\varepsilon_c = E - E_{corr}$ and

$$\eta_{c,2} = \eta_{c,2\ corr} + \varepsilon_c$$

$$i_{c,2} = i_{o,2} \exp\left(\frac{-\eta_{c,2}}{b_{c,2}}\right)$$

$$i_{c,2} = i_{corr} \exp\left(\frac{\eta_{c,2\ corr}}{b_{c,2}}\right) \exp\left(\frac{-\eta_{c,2}}{b_{c,2}}\right)$$

$$= i_{corr} \exp\left(\frac{-\eta_{c,2} - \eta_{c,2\ corr}}{b_{c,2}}\right)$$

$$= i_{corr} \exp\left(\frac{-\varepsilon_c}{b_{c,2}}\right)$$

$$i_{a,1} = i_{corr} \exp\left(\frac{-\varepsilon_c}{b_{a,1}}\right)$$

For cathodic polarisation

$$i_{app,c} = i_{corr} \exp\left(\frac{-\varepsilon_c}{b_{c,2}}\right) - i_{corr} \exp\left(\frac{\varepsilon_c}{b_{a,1}}\right) \ldots (6)$$

For cathodic polarisation E is more negative than E_{corr}; therefore ε_c is a negative term and $i_{a,1}$ decreases as ε_c increases. Thus

$$i_{app,c} = i_{corr} \exp\left(\frac{-\varepsilon_c}{b_{c,2}}\right)$$

Differentiating equation (6),

$$\frac{\delta i_{app,c}}{\delta \varepsilon_c} = \frac{i_{corr}}{b_{c,2}} \exp\left(\frac{\varepsilon_c}{b_{c,2}}\right) - \frac{i_{corr}}{b_{a,1}} \exp\left(\frac{\varepsilon_c}{b_{a,1}}\right)$$

As $\varepsilon_c \longrightarrow 0$

$$\left.\frac{\delta i_{app,c}}{\delta \varepsilon_c}\right|_{\varepsilon_c = 0} = - i_{corr} \left(\frac{1}{b_{c,2}} + \frac{1}{b_{a,1}}\right)$$

In terms of Tafel constant $\beta = 2.303\ b$

$$\left.\frac{\delta i_{app,c}}{\delta \varepsilon_c}\right|_{\varepsilon_c = 0} = i_{corr} \left(\frac{2.303(\beta_{a,1} + \beta_{c,2})}{\beta_{a,1}\ \beta_{c,2}}\right)$$

Since β's are constants, it follows that ε_c varies linearly with applied current near $\varepsilon_c = 0$. The slope of the voltage - current curve at the origin, i.e., $\frac{\delta \varepsilon_c}{\delta i_{app,c}}$ is called the polarisation resistance or R_p.

Thus

$$R_p = \frac{\beta_{a,1}\ \beta_{c,2}}{2.303\ i_{corr}(\beta_{a,1} + \beta_{c,2})} \quad \ldots(7)$$

When cathodic reaction is diffusion - controlled, the corrosion rate is limited by the limiting current density i_{LIM}. Thus $\beta_c = \infty$ at E_{corr} and $\beta_c + \beta_a \simeq \infty$.

The modified equation for R_p reads as

$$R_p = \frac{\beta_a}{2.303\ i_{corr}} \quad \ldots\ldots\ldots \quad (8)$$

Equation (7) is valid only for overpotentials close to the origin as is clear from boundary conditions. Also it indicates essentially a linear

relationship between applied current and overvoltage. The linear relationship between potential and applied current, very close to corrosion potential, exists because the difference between two logarithmic functions of current approximates a linear function when the logarithmic functions are of the same order of magnitude. However, in some instances deviation from linearity even at overpotentials of a few millivolts is possible. Thus in actual practice polarisation resistance is measured most precisely as the slope at the origin of the overvoltage - current curve of which Figure 10 is typical.

Unlike the Tatel extrapolation method, the polarisation resistance method is not likely to affect the subsequent corrosion rate of the material by changing the nature of the surface due to marked changes from the corrosion potential. Because β_a and β_c appear in both numerator and denominator of equation (7) the polarisation resistance is relatively insensitive to changes in either. Instead, very rough estimates of β_a and β_c will give an accuracy of 30 - 50%.

The linear polarisation method can be used to measure galvanic short - circuit current without inserting any instrumentation between the two couple

electrodes. This is because, as stated under the section on galvanic corrosion, when two metals forming the galvanic couple are in electrical contact in the presence of an electrolyte, a galvanic current is established which is equal to the rate of dissolution of the anode in the couple. At overvoltages very close to zero the equation (7) is satisfied since the galvanic coupling results in an equilibrium between two opposing reactions of oxidation and reduction. The absence of instrumentation between the participating electrodes is of special advantage when such instrumentation would disturb the corrosive or physical conditions of the galvanic couple.

Chapter II

EXPERIMENTAL APPARATUS AND MATERIALS

Polarisation cell and electrical circuit

The schematic arrangement of galvanostatic constant current polarisation circuit is shown in Figure 5. The polarisation cell consisted of a Pyrex joint clamped to the test specimen (working electrode) with an O - ring seal. It contained an electrolyte into which the saturated calomel reference electrode (SCE) and auxiliary electrode were immersed (Figure 6). Platinum wire wrapped around the calomel reference electrode was used as auxiliary electrode. The diameter of exposed area was 6 cm giving an area of 28 cm^2. An identical Pyrex joint was positioned below the specimen as in Figure 6 to facilitate clamping. For anodic polarisation the working electrode was connected to the positive terminal of the power source and, for cathodic polarisation, polarity was reversed.

The D.C. power source was used to drive current through the polarisation circuit with an ammeter to measure the current level. The potentiometer measured the potential of the working electrode with respect to the reference electrode

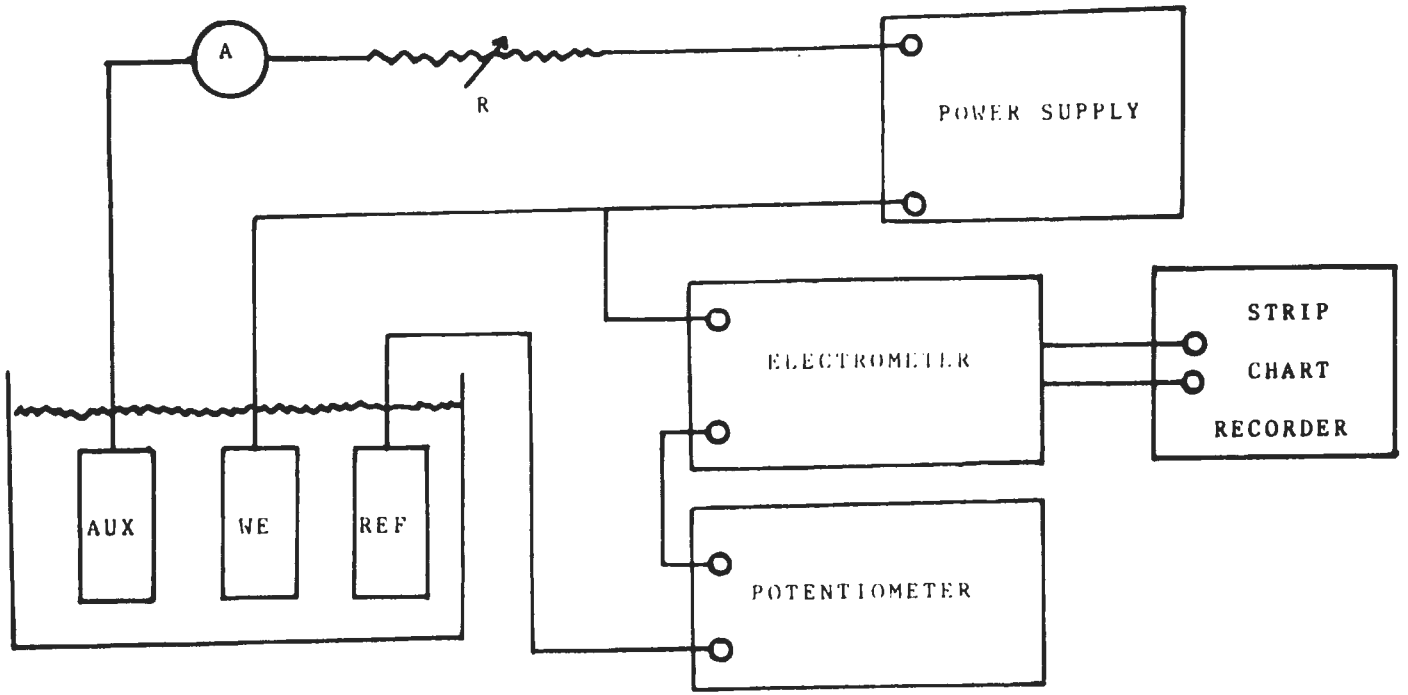

Fig. 5 Galvanostatic circuit

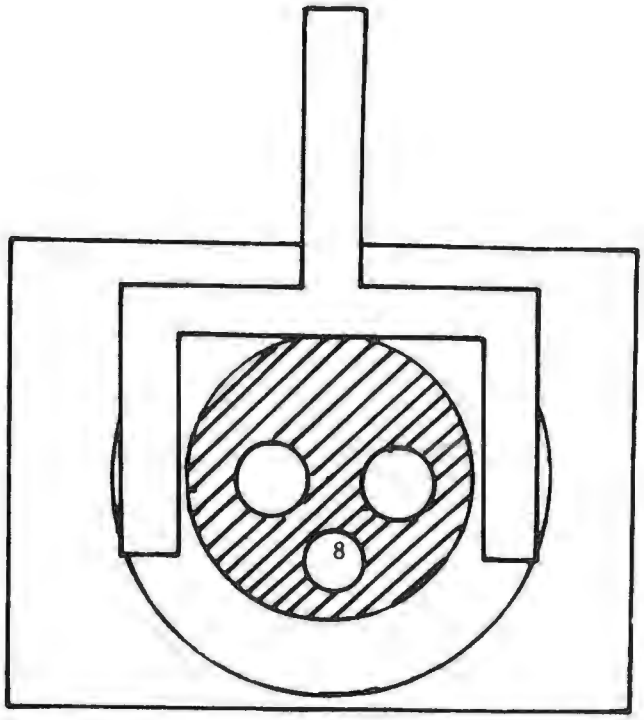

1. Pyrex joint
2. Clamp
3. Specimen sheet
4. Reference electrode
5. Platinum wire auxilliary electrode
6. Gas inlet
7. 'O' ring seal
8. Gas outlet

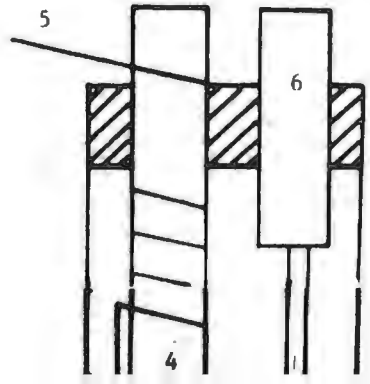

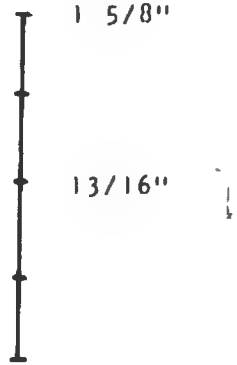

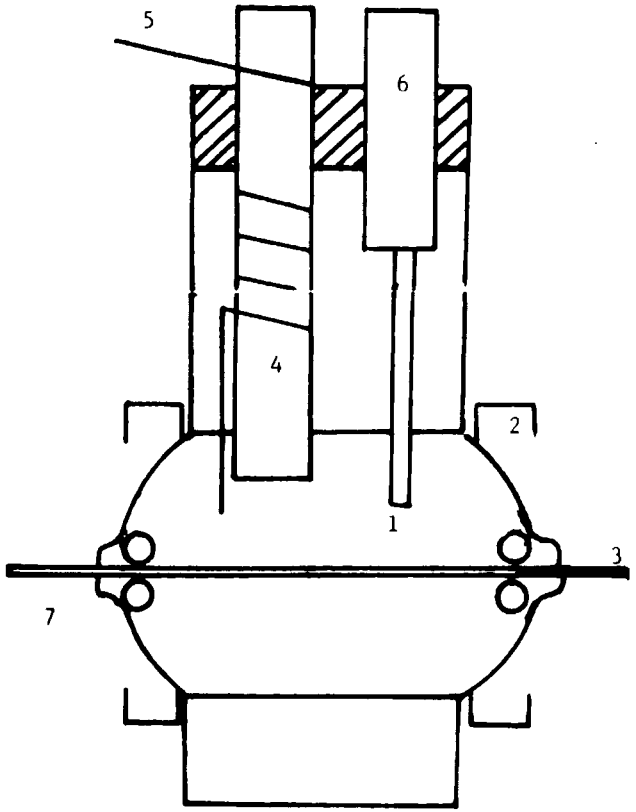

Figure 6. Polarisation cell

13/16"

which was connected to it through an electrometer acting as null detector. For polarisation resistance measurements a chart recorder was connected to the null detector to measure the deviation of working electrode potential from the corrosion potential. Current was lead into the working electrode by alligator clips positioned outside the polarisation cell. A decade resistance box was used in conjunction with the D.C. power source to maintain current at constant levels. Details and specifications of electronic instrumentation are given in Appendix A. When necessary, the solution was deaerated with nitrogen bubbled through the solution with small diameter glass tubing (Figure 6). The gas escaped from the cell through a glass tube having the exit end immersed in a water seal to prevent air leakage into the cell.

Materials and specimen preparation

The coated sheet steels investigated in the present project were designated as follows :-

1) G - 60
2) G - 90
3) Electrogalvanised steel
4) One - side hot dip
5) Nizencote
6) Galvalume

The first four coatings were nominally pure zinc, while the last two were zinc alloys. Sheets were received from Inland Steel Corporation in panels measuring 12 inches by 4 inches by about 0.03 inch thick.

The panels were sheared to 4 inch by 3 inch size and scribes were machined into the surface on a milling machine when required. Scribes measured 1 1/2 inches by 1/8 inch (Figure 7) and, for the sake of convenience, scribe depth was held to half the thickness of the sheet. The area of exposed steel was 1.21 cm^2 giving an area ratio of 1/22 of steel to coating. Scribed specimens were stored in a desiccator to protect the exposed steel surface. Whenever substrate steel was to be studied, the coating was etched away in suitable acid solution followed up by abrasion on belt grinder. Before commencing the experiment, specimens were degreased in benzene and then washed in detergent solution. After rinsing in distilled water, the specimen was dried in an oven at 250^{o}C for ten minutes. The O - ring joint was also separated each time, washed in distilled water, and dried in the oven along with the specimen. After drying, the assembly was set up, clamped, and filled to the required level with

SELF CORROSION

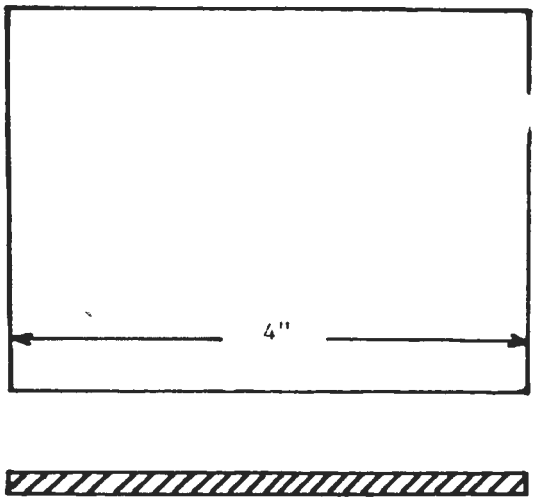

GALVANIC CORROSION

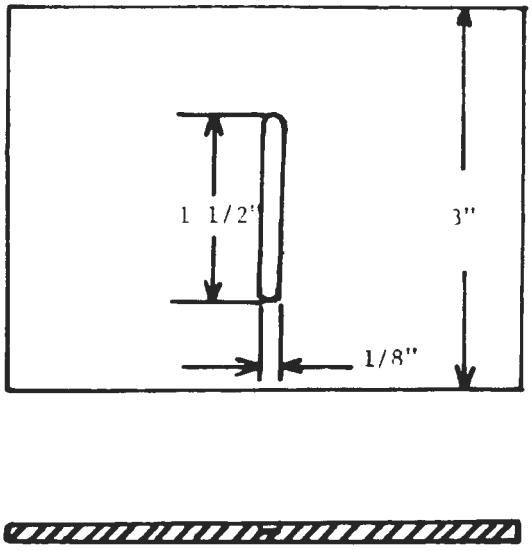

Figure 7. Typical specimens

electrolyte.

The electrolyte consisted of either 0.1 N or 1.0 N sodium chloride solution made up from distilled water and reagent grade salt. Initial experiments were conducted in electrolyte in equilibrium with atmospheric oxygen. Deaeration, when necessary, was carried out by bubbling nitrogen for thirty minutes. A holding time was allowed subsequently for sixty minutes to stabilise the corrosion potential, with nitrogen passing over the top of the solution before the polarisation procedure was initiated.

Chapter III

EXPERIMENTAL PROCEDURE AND RESULTS

Separate specimens of each coating material were subjected to anodic and cathodic polarisation. The coating was stripped off a third specimen which was then subjected to cathodic polarisation to determine the β_c value for steel. The corrosion rate of a fourth specimen was measured by the polarisation resistance method. Effect of galvanic coupling was studied by polarisation resistance measurements on a fifth specimen having a scribe machined into the coating to bare the substrate steel. The above steps were repeated on all six materials in both 0.1 N and 1.0 N sodium chloride solutions, aerated and deaerated.

Polarisation measurements

The polarising current was increased from zero by gradually increasing the voltage output of the power supply and decreasing the resistance of the decade box from its maximum (Figure 5). Current was increased in steps with potential recorded at steady state after ten minutes at each current step.

Typical results for bare steel, G - 90 unscribed, and Galvalume unscribed are shown in Figure 8 for these materials exposed to 1.0 N NaCl

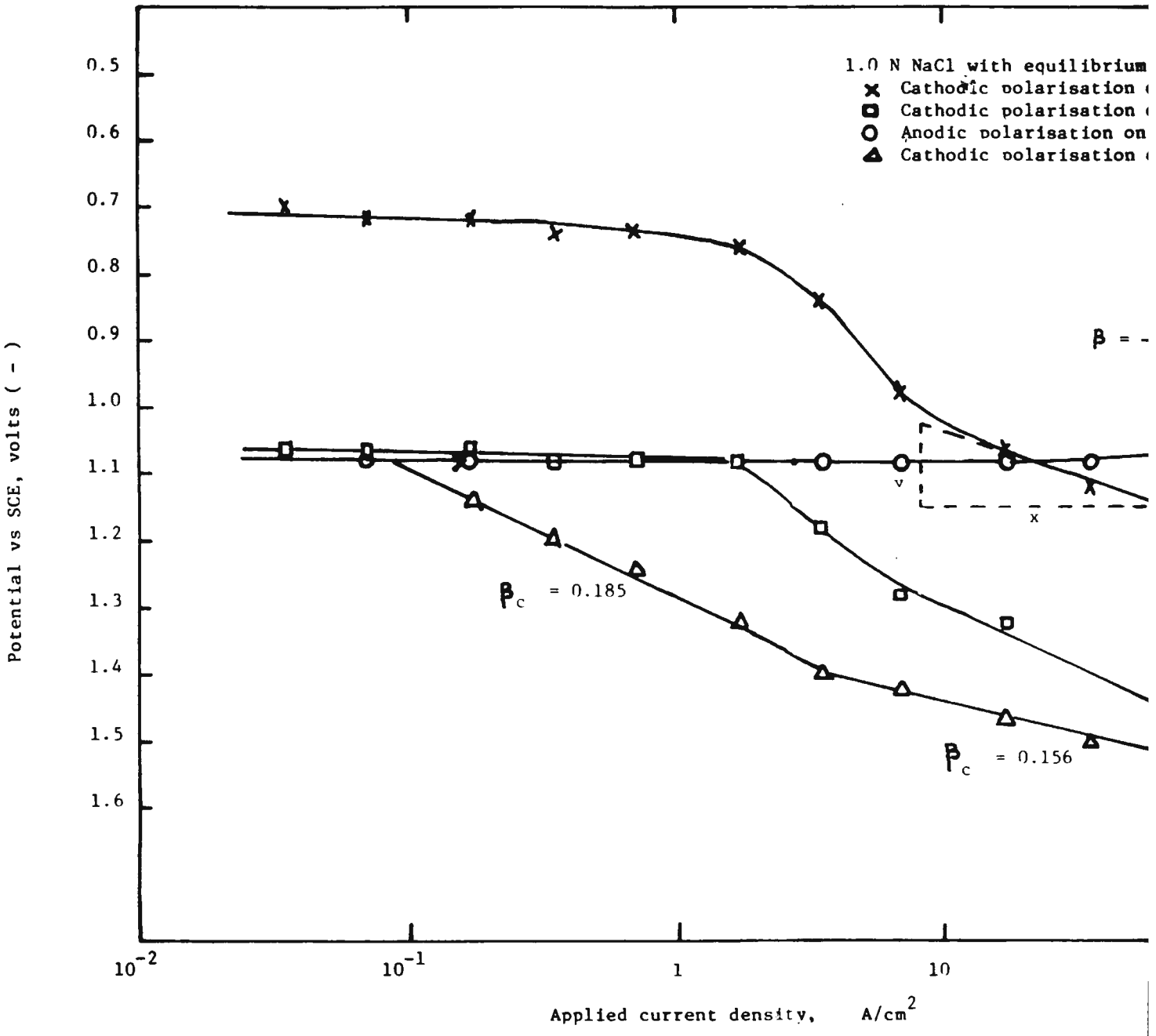

Figure 8. Typical polarisation curves in electrolyte with dissolved oxygen

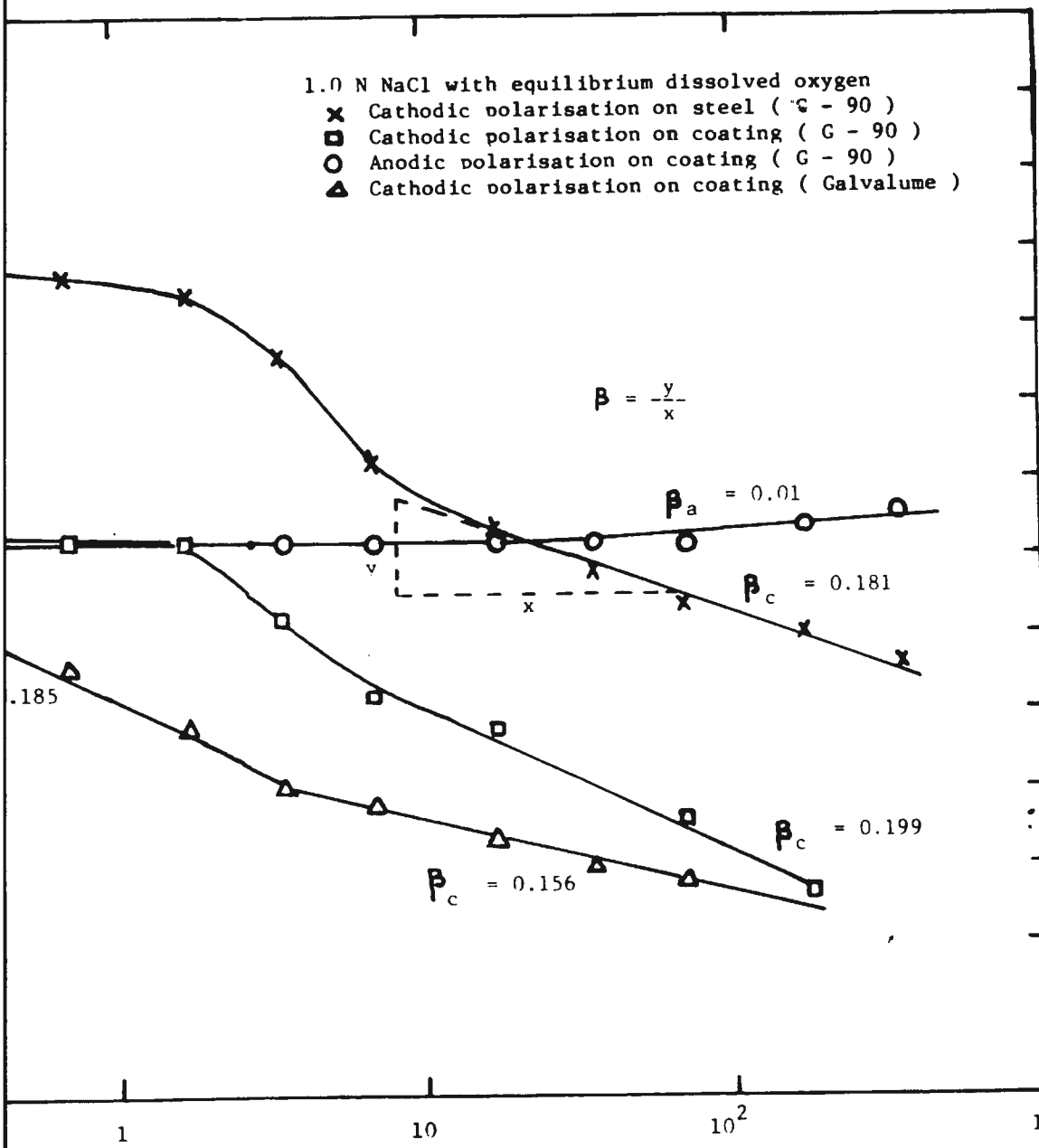

plied current density, A/cm^2

in electrolyte with dissolved oxygen

in equilibrium with ambient atmospheric oxygen. It is notable that the polarising currents for Galvalume are significantly lower than for G - 90, suggesting that Galvalume has a lower corrosion rate. Later replicate polarisation resistance measurements have substantiated such a conclusion. The "knee" in the cathodic curve for steel and G - 90 suggests a contribution by diffusion control of dissolved oxygen. The curves for the same materials in deaerated solution (Figure 9) do not exhibit the "knee" in support of such an interpretation.

The "knee" is absent from the cathodic curve for Galvalume in both cases, indicating activation control for the reduction reaction on this material. In the presence of dissolved oxygen (Figure 8) a change in β_c from 0.185 to 0.156 suggests that two activation controlled processes may be present. Further comments are offered in subsequent DISCUSSION.

Polarisation resistance measurement :-

The polarising current was gradually increased until an initial deviation of only 0.5 to 0.6 mV could be observed on the chart recorder. The current was then maintained until steady state was

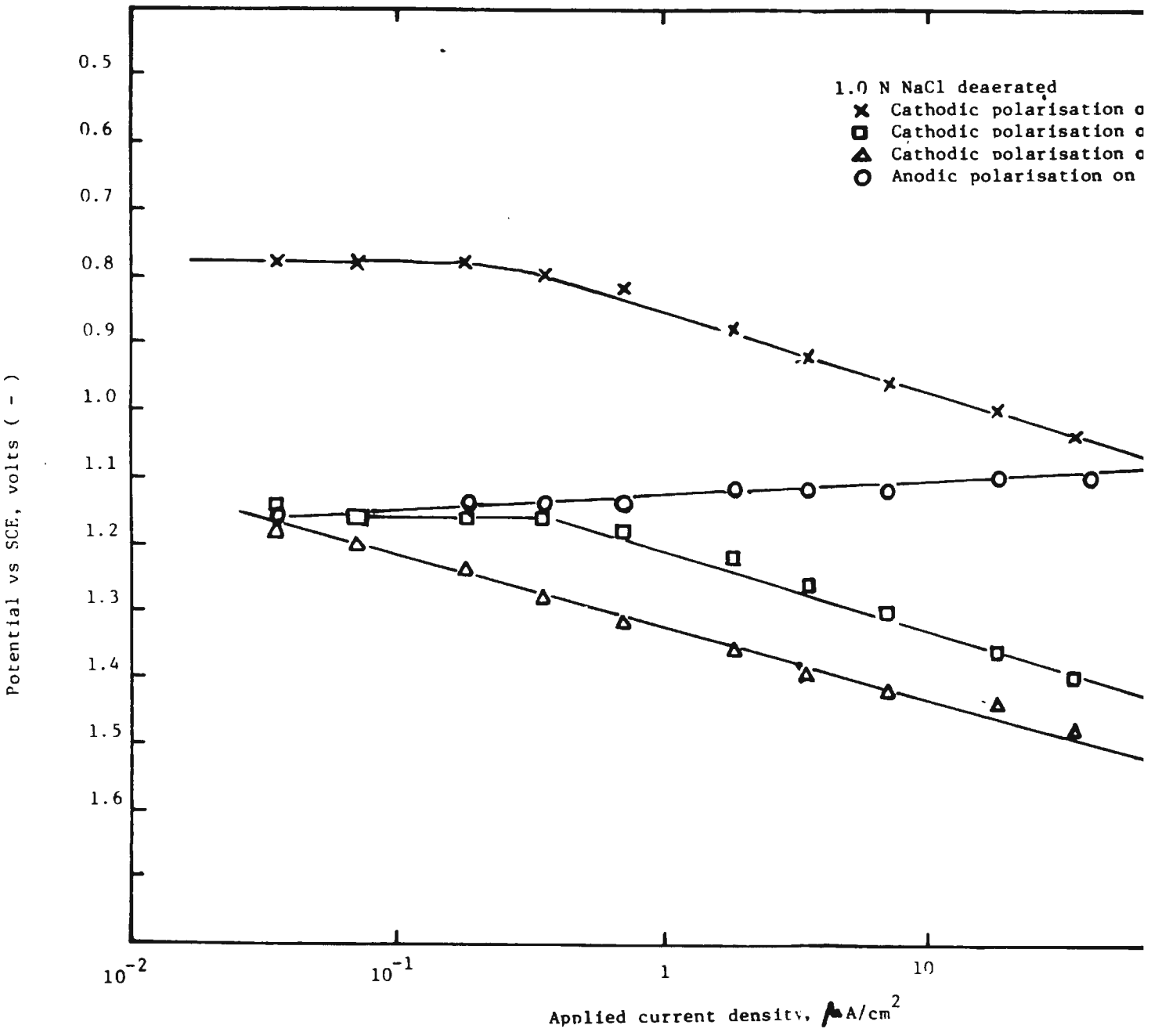

Figure 9. Typical polarisation curves in deaerated electrolyte

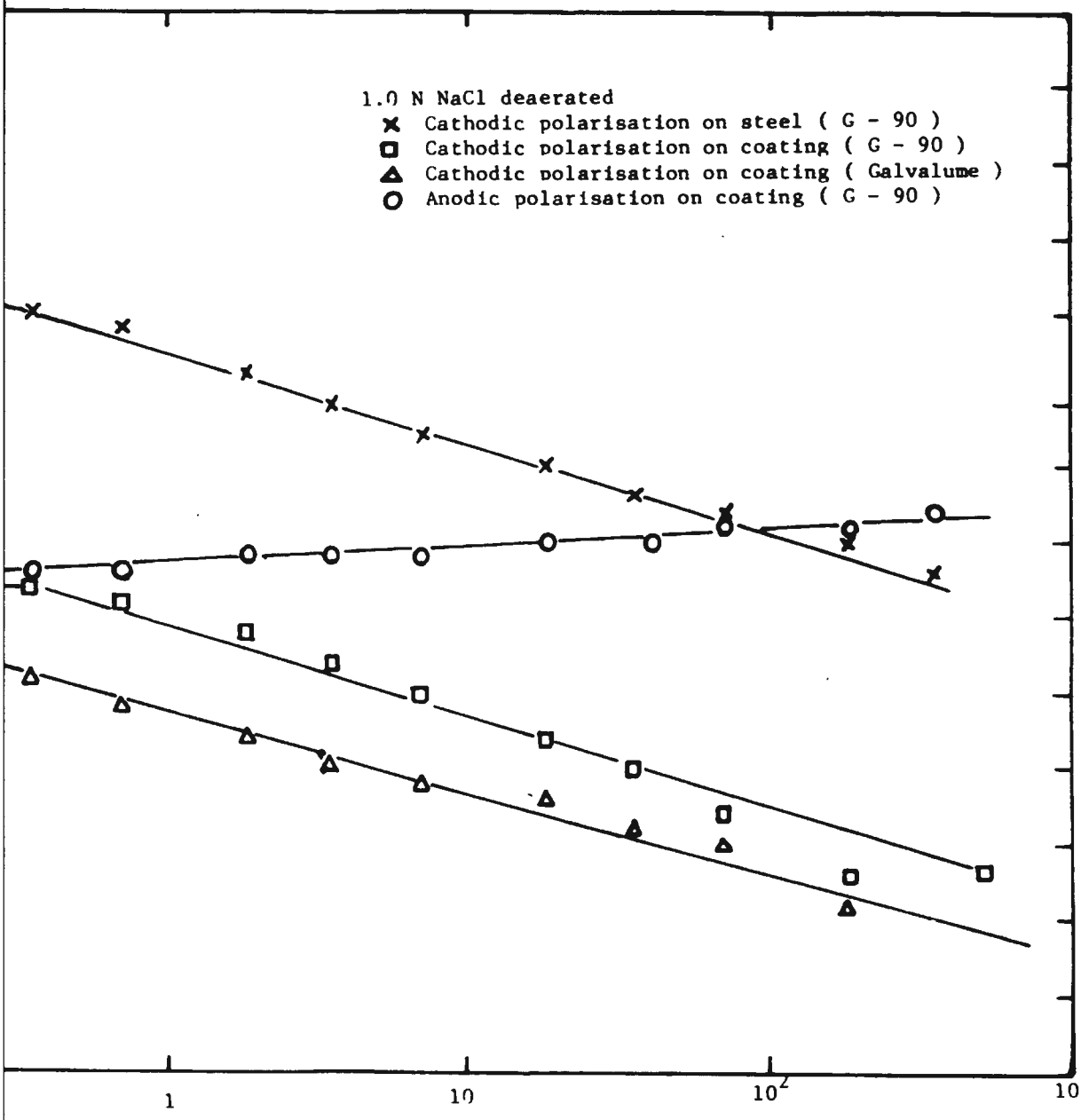

ves in deaerated electrolyte

obtained (usually about one minute), and then adjusted to a value I_1 to obtain a potential change (overvoltage) of 1 - 2 mV. The current was then increased in steps I_2, I_3, I_4, ..., I_n where $I_n = nI_1$. Corresponding overvoltages ε_a, ε_b, ε_c, ..., ε_n were obtained at steady state. A typical tracing taken from a chart record is shown in Figure 10 which shows the procedure for obtaining near steady state values of overvoltage at each current step. The overvoltages ε at each current were plotted in Figure 11 to obtain the polarisation resistance R_p which is the slope at the origin. Note that polarising current rather than current density is plotted in Figure 11. The R_p from such a curve yields a corrosion current I_{corr} when substituted into equation (7) or (8). The corrosion rate (corrosion current density) is then calculated by dividing I_{corr} by the exposed surface area.

The results of polarisation studies of the various materials in 0.1 N and 1.0 N NaCl with equilibrium dissolved oxygen are tabulated in Table I. E_{corr} represents the equilibrium corrosion potential prior to application of current. At higher concentration of electrolyte, E_{corr} was found to take up more noble values for steel while assuming more electronegative values for coatings. β_a and β_c are

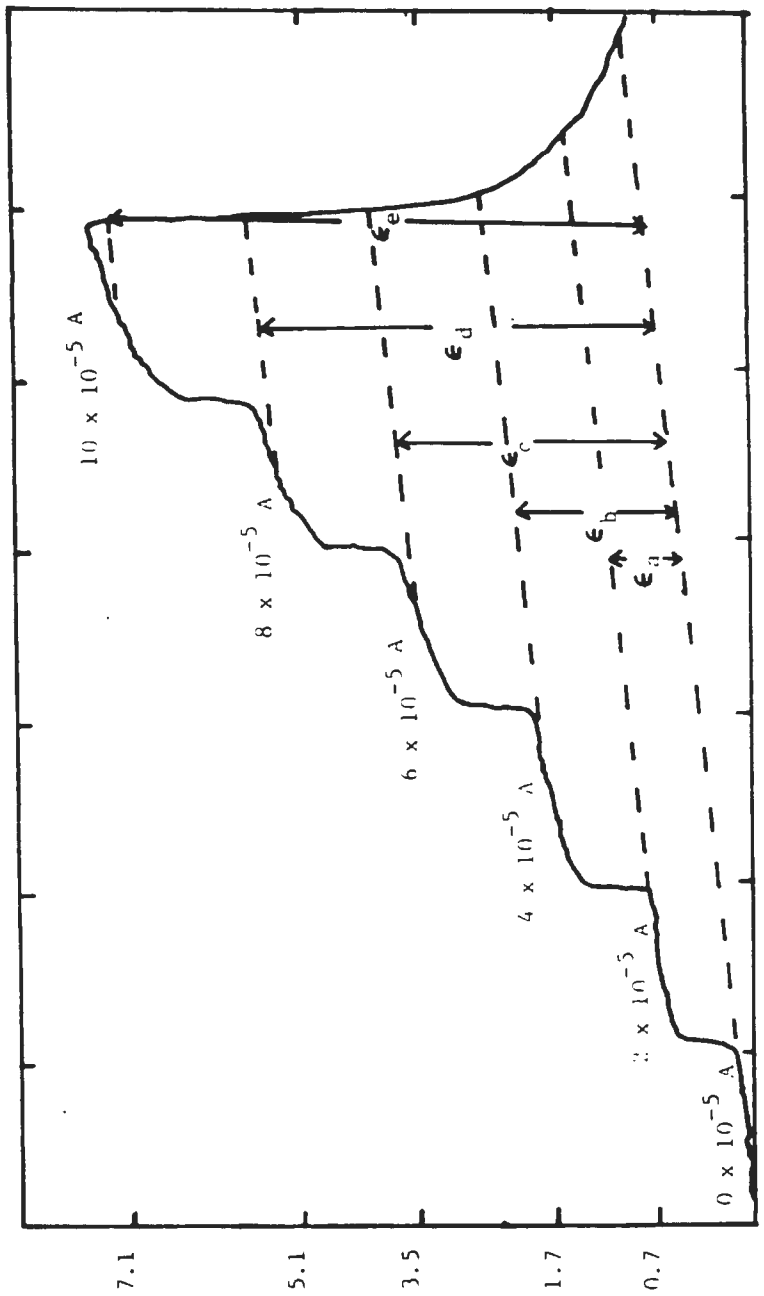

Figure 10. Variation of overvoltage with time at different applied currents

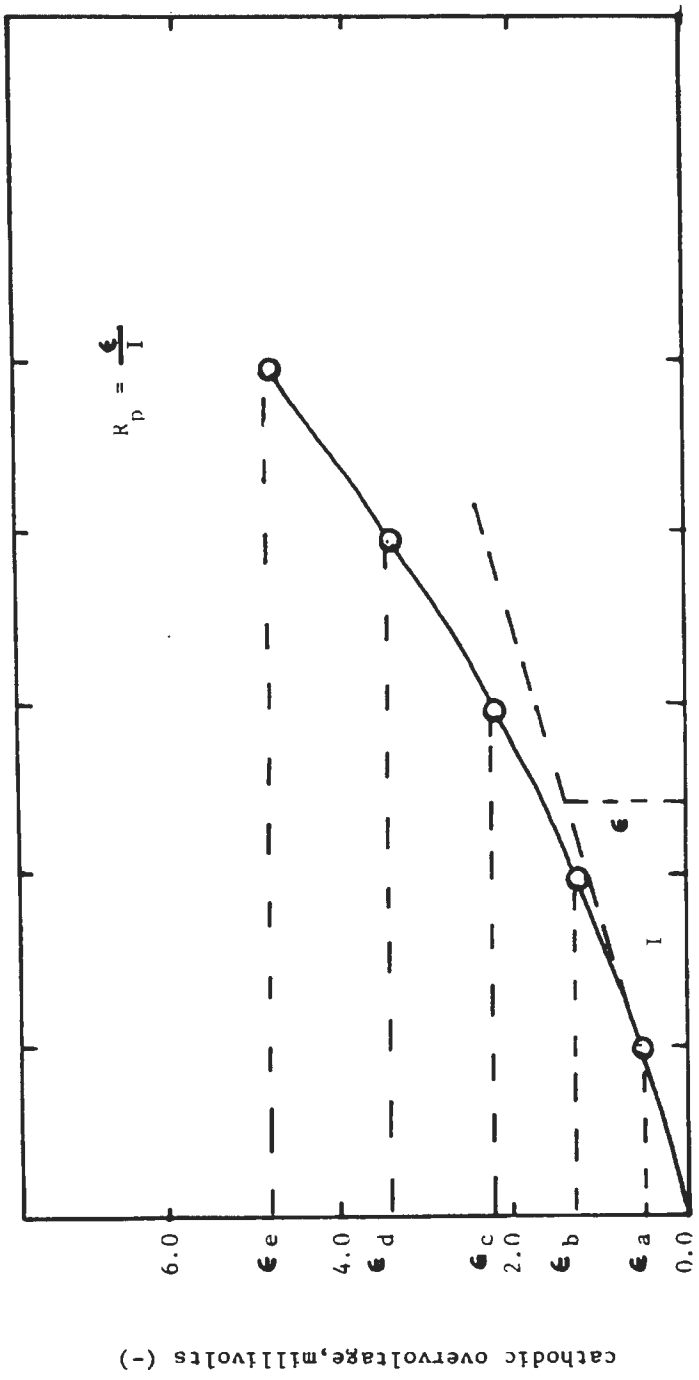

Figure 11. Variation of overvoltage with applied current

Table I

Results of polarisation studies under equi

Material	NaCl concn. N	-Ecorr Steel Volt/SCE	- βc Steel Volt	-Ecorr Coating Volt	-Egalv Scribed Coating Volts	βa Coating Volt	- βc Coating Volt	ig Coating Steel μA/cm²	Coat Rp 10^2 o
G-60	0.1	0.753	0.33	1.044	1.025	0.08	.23	8	2.
	1.0	0.727	0.15	1.077	1.081	0.01	0.156	71	0.
G-90	0.1	0.736	0.185	1.033	1.034	0.027	0.325	18	2.
	1.0	6.699	0.181	1.066	1.072	0.01	0.199	23	1.
Electro Galvanise	0.1	0.702	0.29	1.060	1.032	0.027	0.3061	7	0.
	1.0	0.659	0.175	1.072	1.082	0.014	0.1766	36	0.
One-side hot dip	0.1	0.719	0.231	1.023	1.026	0.028	0.3004	36	0.
	1.0	0.716	0.13	1.067	1.072	0.011	0.2497	57	0.
Nizencote	0.1	0.697	0.17	0.948	.937	0.035	0.28	13	2.
	1.0	0.724	0.17	1.006	.937	0.02	0.2119	16	0.
Galvalume	0.1	0.684	0.21	0.986	.981	0.043	0.12	8	6
	1.0	0.725	0.185	1.049	1.047	0.030	0.1565	18	1

Table I

n studies under equilibrium oxygen.

- βc ating olt	ig Coating Steel μA/cm²	Coating Plain		Coating Scribed		i_{scr}/i_{corr}	Coating Scribed and soaked	
		R_ρ 10^2 ohms	i_{corr} μA /cm²	R_ρ 10^2ohms	i_{scr} μA/cm²		R_ρ 10^2 ohms	i_{scr} μA/cm²
.23	8	2.3	5	1.4	7	1.4		
).156	71	0.35	4	0.3	5	1.25		
).325	18	2.2	2	1.7	2	1.0		
).199	23	1.1	1	0.35	4	4.0	0.3	5
).3061	7	0.6	7	1.4	3	0.4		
).1766	36	0.4	5	0.7	3	0.6		
).3004	36	0.95	5	1.2	3	0.6		
).2497	57	0.65	3	0.7	2	0.7		
).28	13	2.4	2	1.8	2	1.0		
).2119	16	0.91	3	1.6	2	1.5	0.25	11
).12	8	62	0.08	80	0.7	88		
).1565	18	19	0.2	3.6	1.1	5.5	2.8	1.4

the anodic and cathodic Tafel constants measured from polarisation curves as in Figure 8. β values were generally higher in 0.1 N solution. i_g is the current density at the intersection of the cathodic polarisation curve for steel and anodic polarisation curve for the corresponding coating. i_{corr} represents the self - corrosion rate, i.e., the rate at which the coatings corrode when exposed to the electrolyte in the absence of the scribe. i_{scr} is the galvanic current density between the coating and the exposed steel resulting when a scribe is made in the coating. The ratio i_{scr} / i_{corr} indicates the extent of galvanic corrosion.

In the presence of oxygen, the cathodic reaction was diffusion controlled and equation (8) was used to calculate i_{corr} for all unscribed specimens except Galvalume. For the scribed specimen, the cathodic curve for steel is expected to move to the left in comparison to the zinc coatings because area of scribe is only 1 / 22 of the full area exposed during the experiment. This implies that the corrosion rate of the coating must be controlled by activated reduction of water. Therefore equation (7) holds good for scribed specimens. Also, since no "knee" was observed for Galvalume, equation (7) was used for Galvalume.

The polarisation data presented in Figure 9 indicates that cathodic reduction is activation controlled under deaerated conditions because the "knee" is conspicuously absent. The cathodic reaction is assumed to be water reduction which is activation controlled. This assumption is also in line with the earlier discussion on polarisation curves. For this reason equation (7) was used to determine the corrosion rate of all coatings including Galvalume in deaerated electrolyte.

Table II lists the results obtained when the solution was deaerated. The corrosion potentials assume consistantly more electronegative values than those in oxygen - containing solutions. As may be seen, i_{scr} in Table I is less than i_{corr} in several cases. This is contrary to theoretical considerations since, in the presence of bare steel at the scribe, the corrosion rate i_{scr} should be higher than i_{corr} of the unscribed coating as explained under the section on galvanic corrosion. As may be seen from Table II, i_{scr} is consistantly higher than i_{corr} when solution is deaerated.

To determine in a preliminary way the variation in corrosion rate measurements, triplicate measurements of all materials were made in deaerated 1.0 N NaCl solution. The results are presented in

Table II

Results of polarisation studies under deaerat

Material	NaCl concn-N	-Ecorr coating volt	-Egalv Scribed Coating Volt	βa coating volt	-βc coating volt	Coating Plain		C S
						Rρ 10^3 ohms	i_{corr} μA/cm^2	R 10^2 o
G-60	0.1	1.102	1.081	0.026	0.218	1.3	0.3	
	1.0	1.151	1.103	0.028	0.155	1.4	0.2	1
G-90	0.1	1.095	1.066	0.026	0.218	5	0.1	5
	1.0	1.138	1.076	0.028	0.155	20	0.2	1
Electro galva-nised	0.1	1.115	1.053	0.029	0.193	2	0.2	3
	1.0	1.154	1.093	0.028	0.154	1	0.4	1
One-side hot dip	0.1	1.074	1.061	0.023	0.15	4	0.1	5
	1.0	1.16	1.094	0.023	0.17	0.6	0.5	2
Nizen-cote	0.1	.957	.949	0.034	0.167	2.5	0.2	
	1.0	1.022	1.013	0.02	0.163	1.0	0.3	3
Galva-lume	0.1	1.115	.983	0.032	0.124	35	0.01	
	1.0	1.167	1.032	0.03	0.115	16	0.04	

leaeration.

g	Coating Scribed		i_{scr}/i_{corr}
corr $\mu A/cm^2$	$R\rho$ Ω^2 ohms	i_{scr} $\mu A/cm^2$	
0.3	7	1.1	3.7
0.2	1.4	2.3	11.5
0.1	5.5	0.6	6
0.2	1.8	1.8	9
0.2	3.2	1.1	5.5
0.4	1.6	2.1	5.3
0.1	5.5	0.5	5
0.5	2.6	1.1	2.2
0.2	17	0.3	1.5
0.3	3.5	0.7	2.3
0.01	10	0.4	40
0.04	4	0.9	22.5

Table III. The zinc coatings on the whole displayed higher corrosion rates than Galvalume under deaerated conditions, the corrosion rates of zinc coatings, however, exhibiting considerable variance under aerated conditions. This prompted a statistical analysis to ascertain whether it is indeed possible to distinguish between the corrosion rates of two materials with the aim of ranking different materials by electrochemical methods. The procedure, as described by Legault and Dalal (13), was as follows.

Ten runs were conducted on separate specimens of G - 90 and Galvalume in 1.0 N sodium chloride solution under deaeration. Results are presented in Table IV. The overall mean is the arithmetic mean of the ten corrosion rates and the standard deviation represents the amount by which corrosion rate obtained from a test run would statistically deviate from the overall mean. The 95% confidence interval represents the limits within which such a value should lie, from statistical considerations. The confidence interval in Appendix B signifies that there is 95% statistical probability that the measured difference in corrosion rate will lie within the said interval.

The data described above yield corrosion rates of the various coatings but do not indicate

Table III

Triplicate corrosion values in 1.0 N NaCl (Deaerated)

Material	i_{corr} $\mu A/cm^2$			i_{scr} $\mu A/cm^2$			i_{scr} / i_{corr}		
	1	2	3	1	2	3	1	2	3
G-60	0.25	0.35	0.28	2.4	2.1	1.7	9.6	6	6.1
G-90	0.32	0.18	0.14	1.8	2.1	1.8	5.8	11.6	13
Electro-galvanised	0.35	0.35	0.28	1.7	2.1	2.5	4.7	5.8	8.8
One-side hot dip	0.53	0.46	0.32	1.1	1.8	1.4	2.1	3.8	4.4
Nizencote	0.46	0.28	0.14	0.71	0.46	0.42	1.5	1.6	3
Galvalume	0.04	0.04	0.01	0.9	0.9	0.6	25	25	64

TABLE IV

Corrosion current density ($\mu A / cm^2$)

in 1.0 N sodium chloride with deaeration

Run no.	G - 90	Galvalume
1 .	0.304	0.023
2 .	0.182	0.014
3 .	0.137	0.003
4 .	0.304	0.046
5 .	0.182	0.018
6 .	0.273	0.024
7 .	0.273	0.036
8 .	0.219	0.003
9 .	0.182	0.014
10 .	0.156	0.014
Overall mean $\bar{X}$	0.221	0.020
Standard deviation S_x	0.062	0.014
For degree of freedom = 10 - 1 = 9		
t = 1.833 .... (from tables)		
at 95% confidence level		
95% confidence interval	0.221 ±	0.020 ±
	0.114	0.026

the lifetime of the coatings which are dependent also on the coating thickness. To obtain a preliminary indication of coating lifetime, the variation of corrosion potential with time was studied for the various materials (Figure 12). Coupons of each material measuring 1 inch by 4 inches were dipped into 1.0 N sodium chloride solution contained in separate beakers. The corrosion potential was measured every twenty - four hours, keeping solution and specimen unchanged over the entire period of observation. Nizencote, at a very early stage, attained corrosion potential values close to that of steel while G - 90 exhibited values consistantly close to that of zinc before reverting to corrosion potential of steel at the end of almost two weeks. No notable change was observed in Galvalume even after two weeks.

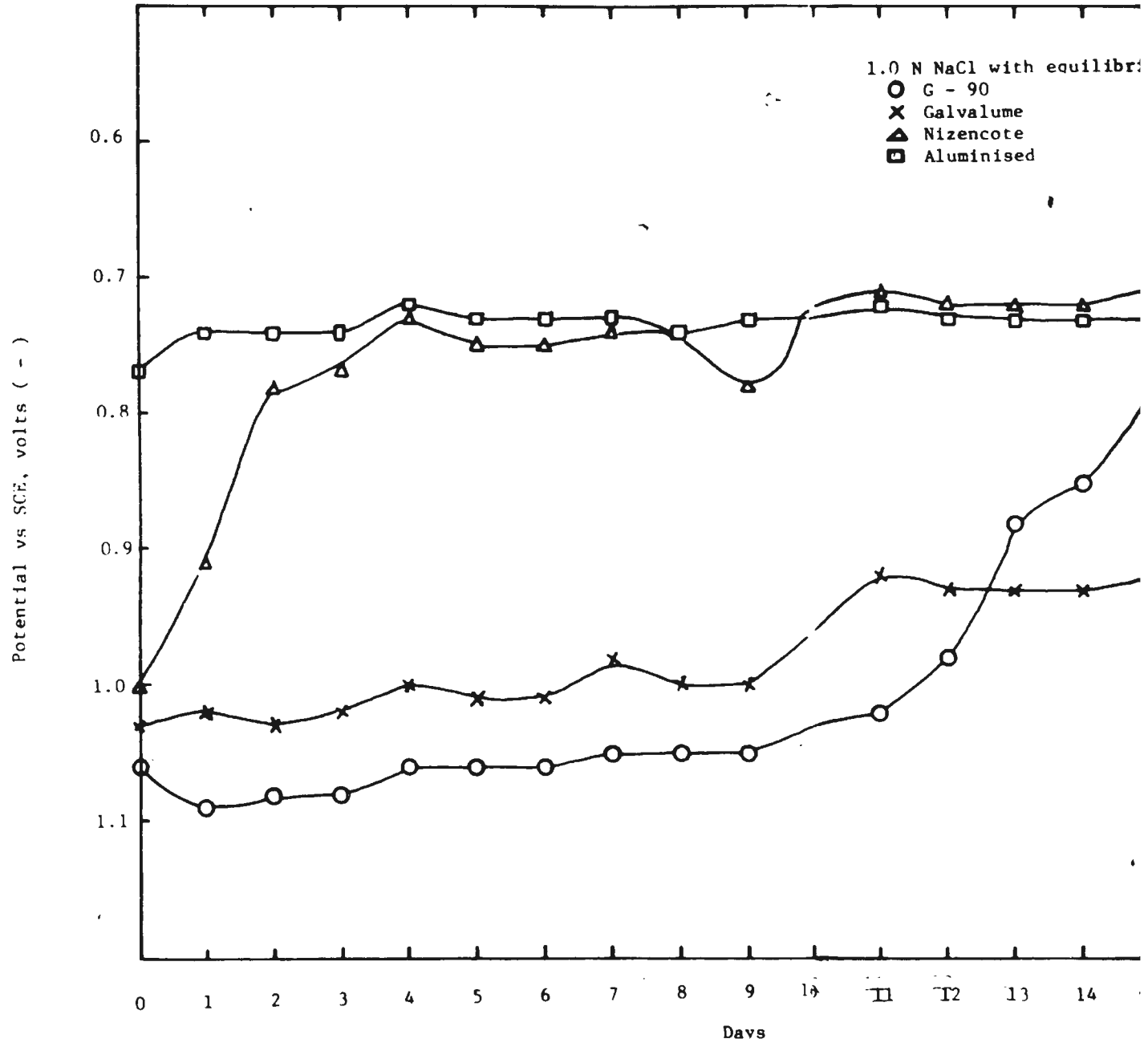

Figure 12. Variation of corrosion potential with time

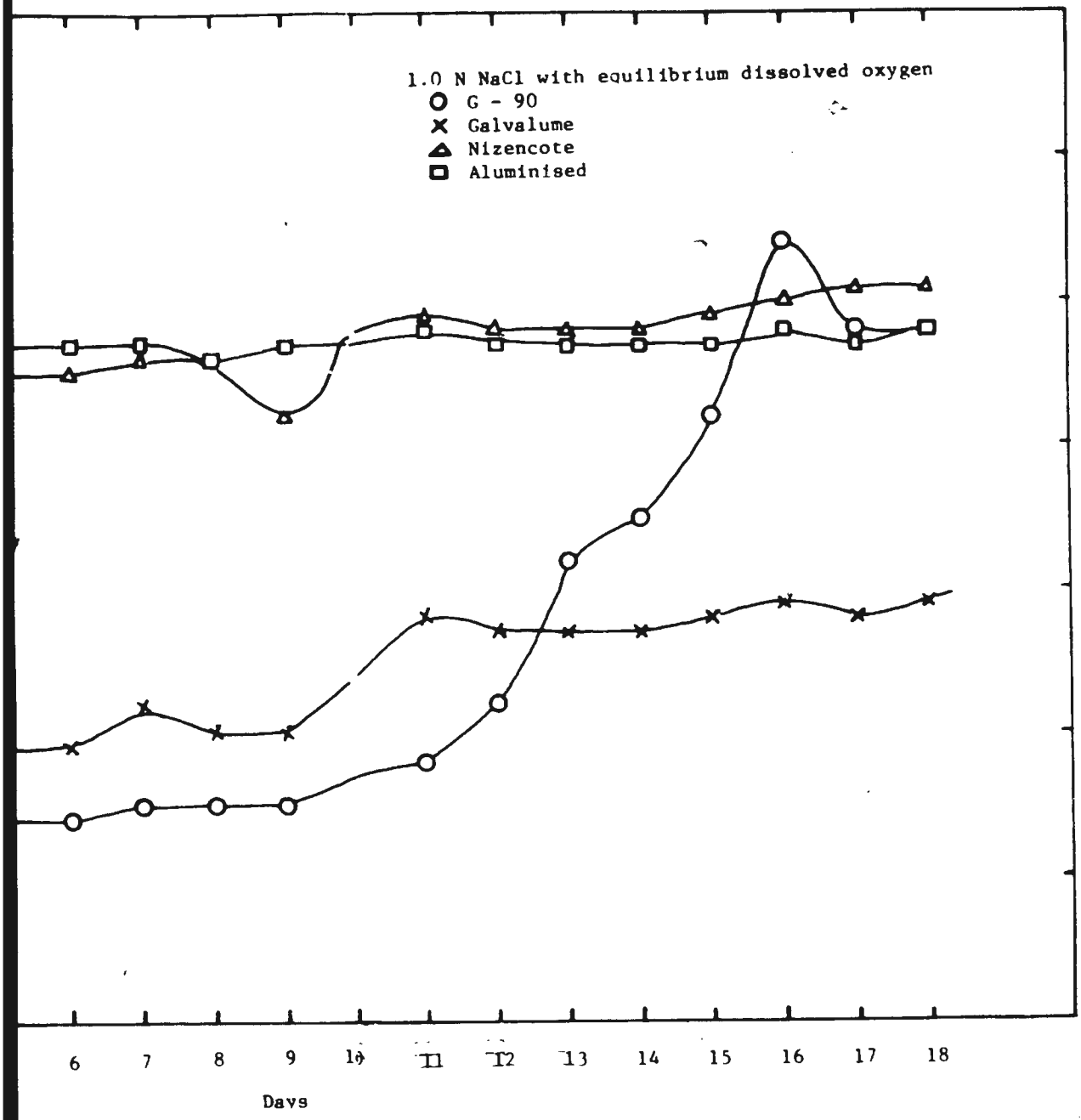

ion potential with time

Chapter IV

DISCUSSION

1. Polarisation data

The shape of the cathodic polarisation curve for steel and G - 90 may be explained on the basis of mixed activation and concentration polarisation in the current range employed. Consider the two reactions

$$2H_2O + 2e^- = H_2 + 2OH^-$$

$$O_2 + 2H_2O + 4e^- = 4OH^-$$

If indeed oxygen reduction limited by concentration polarisation occurs at lower currents, the concentration overvoltage would result in a curve similiar to Figure 2. Also the water reduction at higher current ranges would give rise to a curve similiar to Figure 3 wherein activation polarisation is controlling. Diffusion control is often experienced in the reduction of dissolved oxygen because of the limited solubility (8 ppm maximum) of oxygen in aqueous media. Activation control for reduction of water to H_2 would be expected due to the unlimited supply of H_2O molecules. Combining the two curves could result in a curve as shown in Figure 13 showing the characteristic "knee". Similiar conclusions were reached in earlier work (12)

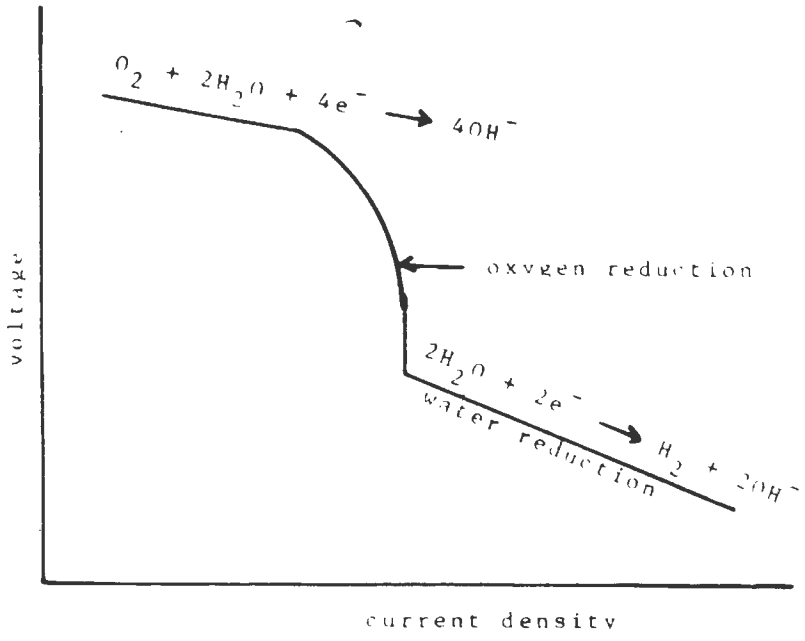

Figure 13. Theoretical model for cathodic polarisation curves.

involving different metals in chloride solutions.

Further verification is shown in Figure 14. A trial - and - error value of limiting current i_{LIM} for oxygen reduction is selected and marked by the vertical dashed line ab. The water reduction portion of the cathodic polarisation curve is defined by the dashed line beyond E_{corr} to e. The sum of reduction curves ab and cde between d and a is given by the line dfa. At potentials active to d reduction of water to hydrogen predominates along the line cd. At potentials noble to f, the reduction of dissolved oxygen would predominate.

The anodic dissolution process for the zinc coating is given by fitting the dashed line gh to the anodic data at high current density. The applied current density at any given potential is derived from

$$i_{app} = i_{red} - i_{ox}$$

where i_{red} is the total reduction current density on the line afd and i_{ox} is the total oxidation current density on the line gh. The three currents are marked at - 1.1 volt on Figure 14. The solid line in Figure 14 is derived by finding i_{app} at various potentials between E_{corr} and point c. The solid line conforms well to the data points and is near to the shape of polarisation curves drawn through the points.

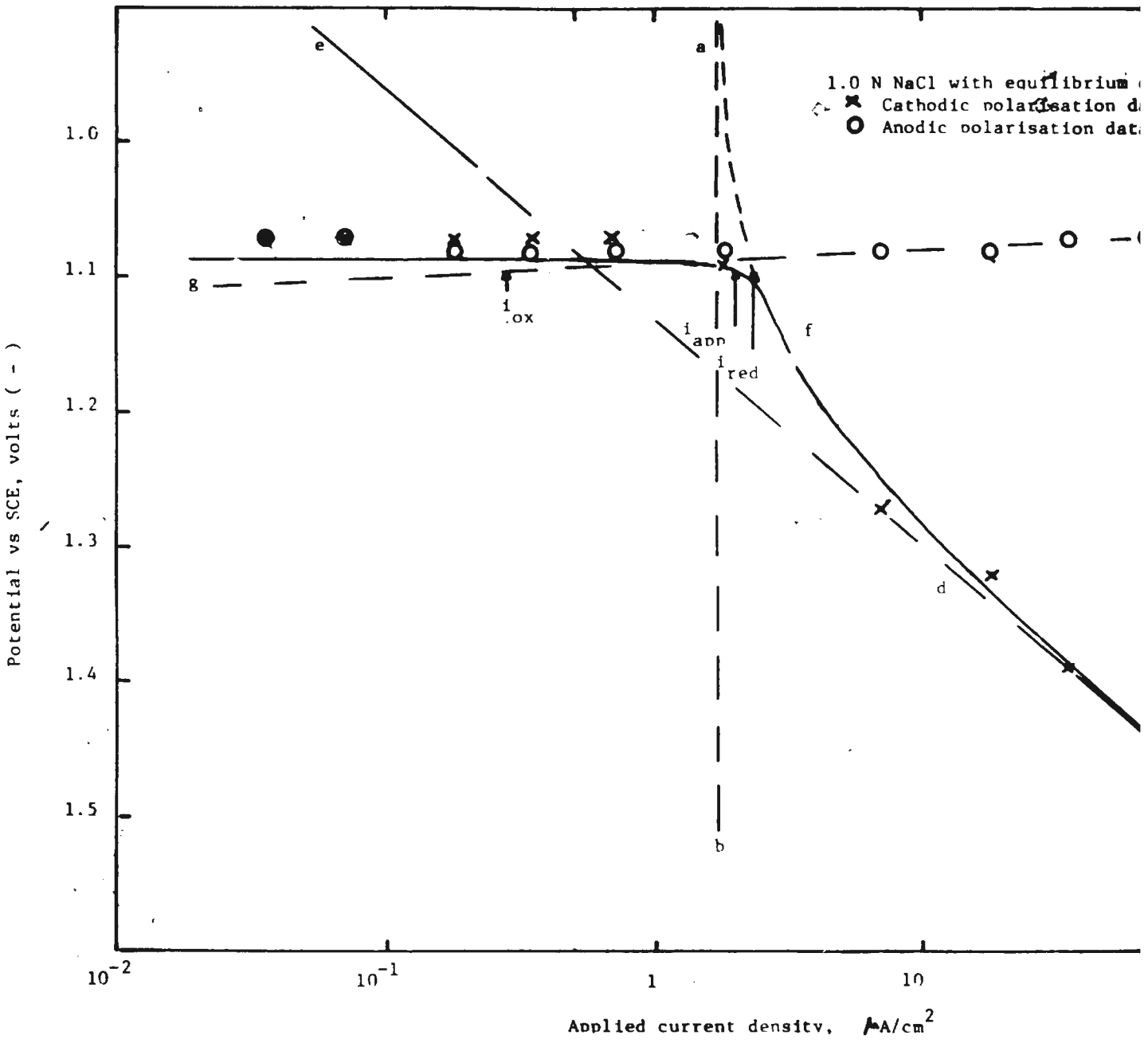

Figure 14. Construction of "knee" in polarisation curve

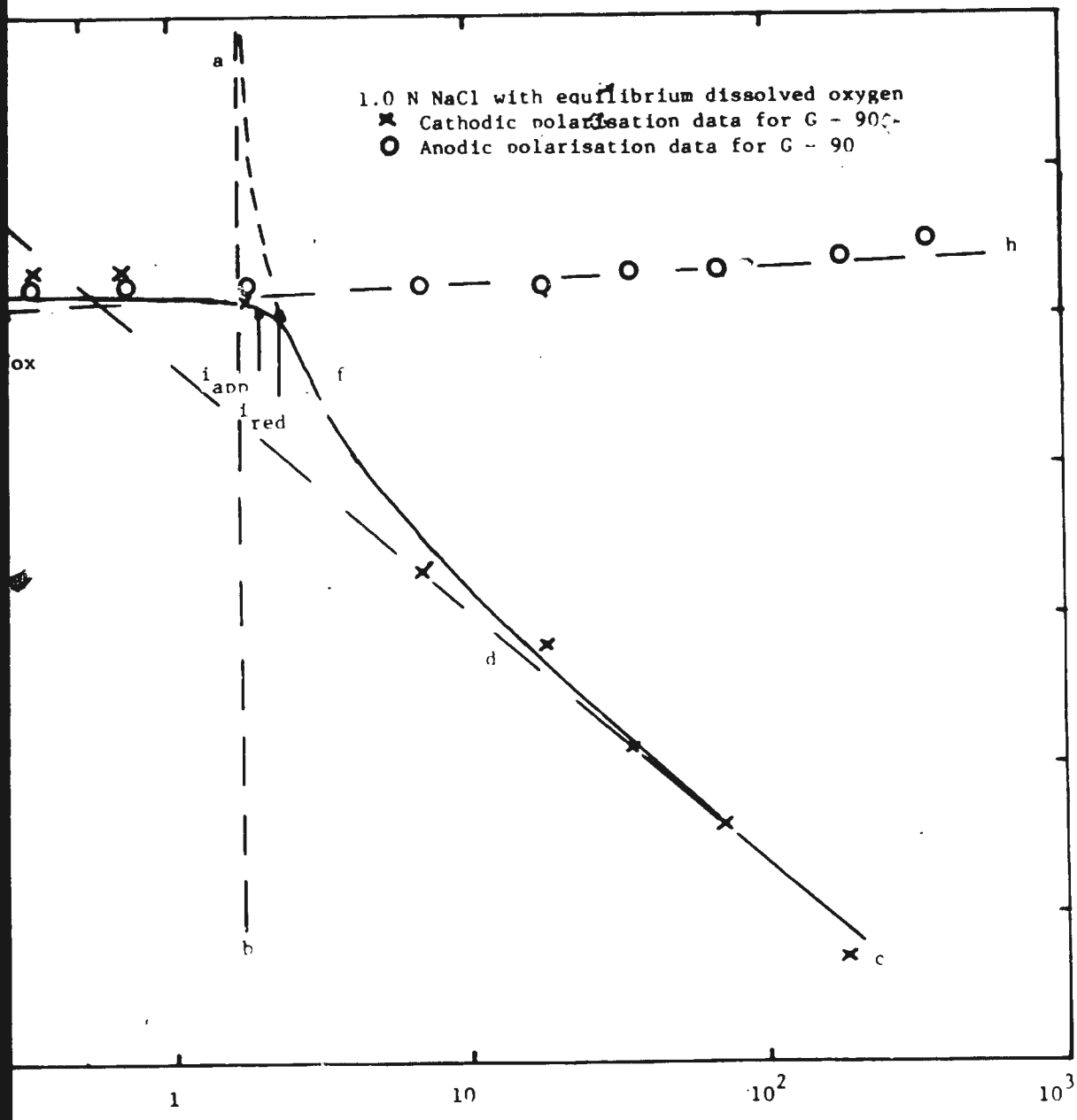

n polarisation curve

The fact that the solid line closely follows the data points confirms the initial assumption that corrosion is controlled by combined reduction of dissolved oxygen and water to evolve hydrogen.

The "knee" was exhibited by all coatings except Galvalume. It would appear that the cathodic reaction is activation controlled in this instance. Galvalume exhibited virtually no change in corrosion potential with time as shown in Figure 12. An explanation for the consistantly isolated behaviour of Galvalume is in order. The coating material (nominal composition : 55% Al, 43.4% Zn, 1.6% Si) in this case is an alloy of zinc and aluminium in roughly equal parts. The E_{corr} values of this material being close to that of pure zinc indicates the contribution of zinc in the coating and the lower corrosion rate of the coating is probably a reflection of aluminium content. This points to the possibility that the formation of an aluminium - oxide - bearing film on the surface slows down the migration of electrons to outer surface and transfers control to an activation process which is slower than the maximum rate of diffusion of dissolved oxygen to the interface from the bulk solution.

2. Polarisation resistance data

- Corrosion current densities from polarisation

resistance data for G - 90, Galvalume, and Nizencote after overnight (twenty hours) exposure are shown in column 12 in Table I. For separate specimens of G - 90 exposed to solution for thirty minutes and twenty hours, the 5 $\mu A / cm^2$ value is approximately same for both. Much of the protective nature of Nizencote was lost after the twenty - hour exposure, since i_{scr} is quite high at 11 $\mu A / cm^2$. i_{scr} is still nearly the same after twenty hours (1.4 $\mu A / cm^2$) as it was after thirty - minute exposure (1.1 $\mu A / cm^2$) for Galvalume. Therefore these data suggest that the initial thirty - minute exposure data gave an accurate indication of the longer - term electrochemical behaviour of the coating.

The i_{scr} values should theoretically have been higher than i_{corr}. As explained in Figure 4, the scribe exposes the substrate steel and results in a higher measured current for the coating due to galvanic coupling to a nobler metal. The coating becomes the sacrificial anode to protect the exposed steel. However, the metal area over which oxygen is reduced is still the same when the scribe is present. Therefore the i_{LIM} should be the same for both scribed and unscribed specimens (Figure 15). i_{scr} is sometimes greater or less than i_{corr} due to the inherent variability of i_{LIM} and this explains the values given

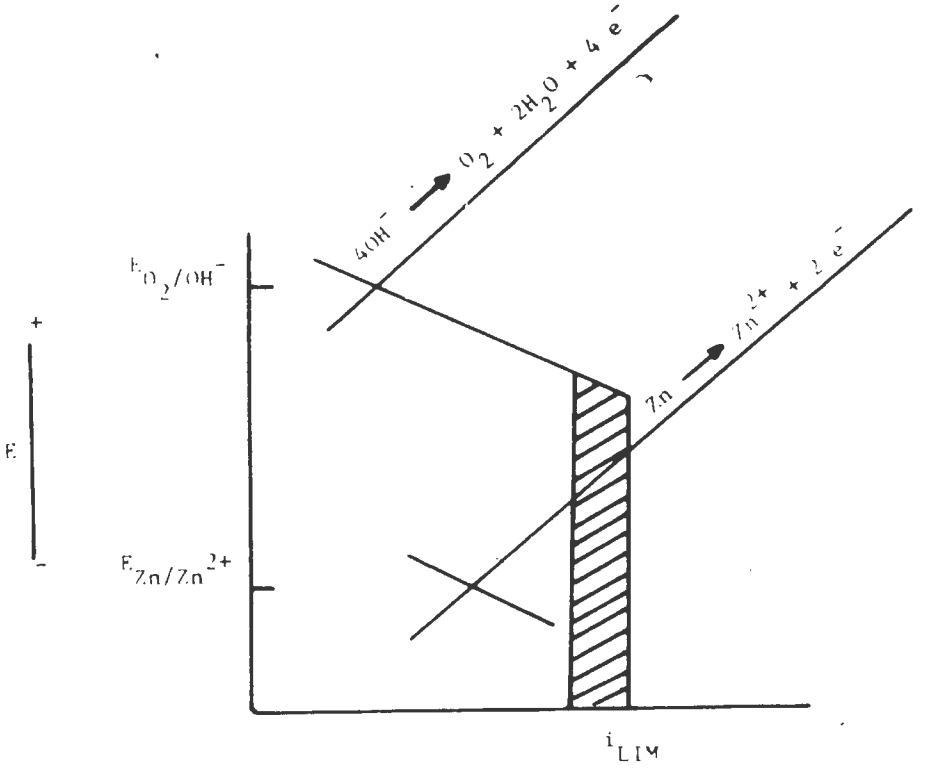

Figure 15. Corrosion behaviour in the presence of equilibrium dissolved oxygen

by Table I in the presence of equilibrium dissolved oxygen. The variability of i_{LIM} is inherent due to variations in dissolved oxygen concentration and slight variations in rate of convection. Bubbling compressed air through the electrolyte did not improve the variability of i_{corr}. The results were essentially the same as for solutions in equilibrium with atmospheric oxygen. Thus they have not been repeated here for brevity.

Tables I and II give the corrosion current densities under equilibrium dissolved oxygen and deaerated conditions in 0.1 N and 1.0 N sodium chloride solutions. The i_{scr} values are definitely higher than i_{corr} under deaeration, as expected. In the absence of dissolved oxygen, the two redox reactions are

$$Zn = Zn^{2+} + 2\ e^-$$

$$2H_2O + 2\ e^- = 2OH^- + H_2$$

Figure 16 illustrates the mechanism of unscribed and scribed coating. Note that in the case of scribed specimen there is a second reduction reaction, namely the reduction of water on steel and as a result the total reduction curve is the sum of water reduction on the two different metals. It is assumed that water reduction is more rapid on the exposed steel surface than on the same area of coating which was removed by the scribe.

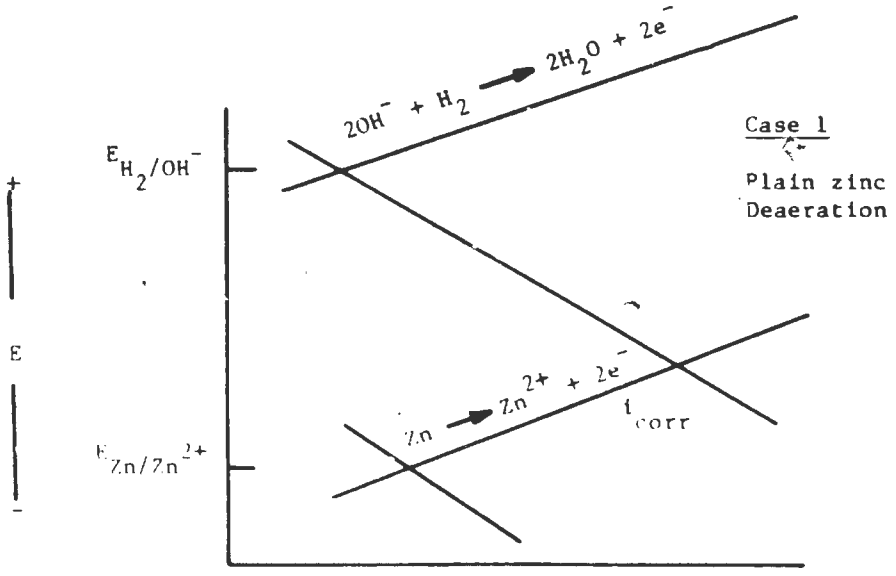

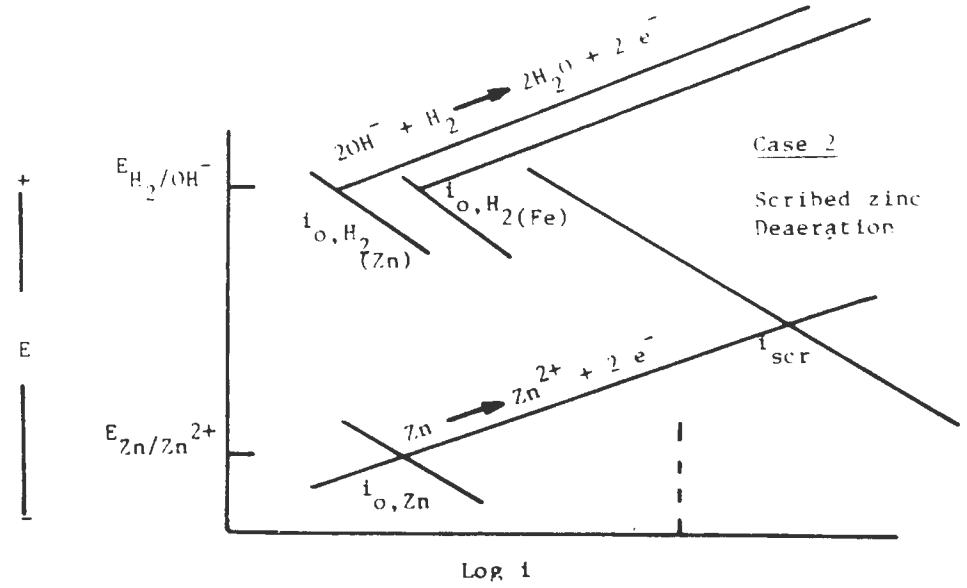

Figure 16. Corrosion behaviour under deaeration

It would be observed from Figure 8 that the cathodic polarisation curve for Galvalume changes slope and this change is not observed in Figure 9 under deaerated conditions. This indicates that under aerated conditions both oxygen and water reduction take place, the difference being that in the case of Galvalume the oxygen reduction is activation controlled even under aerated conditions.

The statistical analyses presented in Table IV and Appendix B highlight the difference in corrosion behaviour between G - 90 and Galvalume. The 95% confidence interval indicates not only that it is possible to assign statistical limits for the corrosion behaviour of either material but also brings about the significant difference between the two materials as regards to corrosion rates. It should be noted that the interval for true difference in corrosion behaviour does not include the value zero. This indicates that it should be possible to discriminate between the two materials on the basis of an electrochemical method.

Figure 12 provides an indication of the longer - term behaviour of coatings where the thickness of the coating has a significant role. This is evident from the difference in behaviour between

Nizencote which is thinner and the other coatings. This aspect was not further explored in this project and requires more in - depth investigation.

Chapter V

SUMMARY

In both aerated and deaerated solutions bare steel is polarised and protected cathodically by coupling to zinc and zinc alloy coatings. In aerated solutions, the corrosion rates of coatings are considerably higher and coating lifetime may be expected to be considerably lower for given coating thickness. Aluminium - zinc (Galvalume) coatings exhibited considerably lower corrosion rates yet were still successful in cathodically protecting bare steel surfaces. Lower corrosion rates of Galvalume in both aerated and deaerated solutions correlate with apparent activation controlled reduction of both water and dissolved oxygen.

Measurements in aerated solutions were rather unpredictable. The corrosion rate in the presence of a scribe in the coating i_{scr} could be greater or less than the corrosion rate i_{corr} of the unscribed coating. Presumably the variability is due to changes in dissolved oxygen content in the chloride solution. However, it has been impossible to quantitatively relate i_{corr} to dissolved oxygen.

The corrosion rates, i_{corr}, were decreased

by several orders of magnitude when dissolved oxygen was removed by sparging with pure nitrogen. The variability of i_{corr} was reduced much below the increase caused by the presence of a scribe. Thus i_{scr} was consistantly greater than i_{corr} in deaerated solutions. The steel exposed by a scribe in the coating has a greater rate of reduction than the coating material which it replaces, resulting in higher total corrosion rate in the presence of a scribe.

There seem to be no sensible differences between the various pure zinc coatings; i.e., G - 60, G - 90, electrogalvanised steel, and one - side hot dip; on the basis of polarisation resistance measurements. The electrochemical properties (including corrosion rate i_{corr}) of these nominally pure zinc coatings appear to be quite similar.

Coating lifetime on steel is at least partially a function of thickness. In a preliminary way, simple corrosion potential measurements have been shown to be sensitive to the loss of the coating. Further work is recommended to assess electrochemical procedure for evaluating longer - term performance and lifetime of coatings on steel sheet.

The electrochemical methods show great promise in evaluating the alloy coatings

(e.g. :- Nizencote and Galvalume) in which electrochemical properties differ substantially from pure zinc. Nizencote does not show a substantial reduction in i_{corr} below that of zinc coatings and could not be recommended in preference to pure zinc coatings. Galvalume shows very good properties : very low i_{corr} and a very high ratio of i_{scr} / i_{corr} in both aerated and deaerated solutions.

Appendix A

APPARATUS

The experimental set - up consisted of

1) D.C. power source
2) decade resistance box
3) electrometers
4) potentiometer
5) ammeter

1) D.C. power source :-

Although batteries may be used, D.C. power supplies are more convenient to use over long periods of time at steady output voltages. Also the lack of A.C. rinnle is important because polarisation behaviour is distorted in the presence of small superimposed alternating voltages. A Heath - Schlumberger power supply, Model no. SP 2710, was used in the present project. It had an output range of 0 - 30 volts.

2) Decade resistance box :-

Decade box is used in between power source and polarisation cell to maintain a steady current. A Phipps & Bird decade box, Model A236, with an accuracy of 1% and power rating of 10 watts was used. By using toggle switches, it was possible to vary the resistance

included in the cell.

3) Electrometer :-

An electrometer is an electronic voltmeter with extremely high input impedance. The primary reason for using high input impedance voltage measuring circuits is to avoid drawing current which would polarise the reference electrode (14). Keithley electrometer, Model 610C, having an input impedance of 10^{14} ohms, was used as null detector. Its function was to compare the potentiometer standard voltage with that of the working electrode through a reference electrode.

4) Potentiometer :-

Electrode potential measurements were done with a compact portable potentiometer. Used in this project was a Biddle potentiometer, Model 72 - 312, with a measuring range between 0.11 to 1.161 volts. This instrument was powered by a battery.

5) Ammeter :-

It is imperative in electrochemical measurements that no current be drawn from the system by the equipment for measurement itself. With this in view, an electrometer was used to measure currents. Further advantage is the wide range of currents measured by this instrument. It differed from the null detector in that it was solid state battery - operated whereas the latter was line - operated. Battery

operation ensures the absence of interference from line - operated null detector. Keithley Instruments, Model 602, with a current range from 10^{-11} to 1 ampere was used.

APPENDIX B

Confidence interval for the true difference in corrosion behaviour between G - 90 and Galvalume :-

$$\text{Confidence interval} = \bar{X}_g - \bar{X}_{ga} \pm t \times \sqrt{\text{estimated variance of } (\bar{X}_g - \bar{X}_{ga})}$$

where $\bar{X}$ = sample mean

$$t = \frac{\text{data point - population mean}}{\text{standard deviation}}$$

For degree of freedom $(10 - 1) + (10 - 1) = 18$

$t = 1.734$ .. from t-distribution table for 95% confidence level

$$\text{estimated variance of } (\bar{X}_g - \bar{X}_{ga}) = s_p \left(\frac{1}{n_g} + \frac{1}{n_{ga}}\right)$$

where $$s_p^2 = \frac{(n_g - 1)s_g^2 + (n_{ga} - 1)s_{ga}^2}{(n_g - 1) + (n_{ga} - 1)}$$

where n = number of data points in a sample

s = standard deviation

95% Confidence Interval : 0.202 ± 0.035

LIST OF REFERENCES

1. Fontana M.G. and Greene N.D. Corrosion Engineering, McGraw - Hill Inc. (1978), 1

2. Stern M. and Weisert E.D. Experimental Observations on the Relation between Polarisation Resistance and Corrosion Rate. ASTM Proceedings, 59, (1959), i280+

3. Standard Method of Salt Spray (Fog) Testing. ASTM B117 - 73

4. Standard Recommended Practice for Laboratory Corrosion Testing of Materials. ASTM G 31 - 72

5. Standard Recommended Practice for Conducting Atmospheric Corrosion Tests on Metals. ANSI / ASTM G 50 - 76

6. Standard Recommended Practice for Conducting Surface Seawater Exposure Tests on Metals and Alloys. ANSI / ASTM G 52 - 76

7. Jones D.A. Anodic Polarisation of Anodised Aluminium. Corrosion, 25, (1969), 297

8. Chance R.L. and France W.D. Anodic Polarisation Characterisation of Phosphated Steels. Corrosion, 25, (1969), 239

9. Potter E.C. Electrochemistry. Cleaver - Hume. (1961)

10. Mansfeld F. The Polarisation Resistance Technique for Measuring Corrosion Currents. Advances in

Corrosion Science and Technology, vol. 6, Plenum Press, (1976), 163

11. Jones D.A. Monitoring Galvanic Short - Circuit Currents. Electrochemical Technology, (1968), 241

12. Evans U R., Bannister L.C., and Britton S.C. The Velocity of Corrosion from Electrochemical Standpoint. Proceedings of Royal Society, A131, (1931),355

13. Legault R.A. and Dalal J.G. The Statistical Analysis of Atmospheric Corrosion Data. International Symposium on Atmospheric Corrosion, October 1980

14. Greene N.D. Experimental Electrode Kinetics, Rensselaer Polytechnic Institute, (1965)